OXFORD GENETICS

GENETICS, 2025, iyaf235
https://doi.org/10.1093/genetics/iyaf235
Advance Access Publication Date: 1 November 2025
Investigation

Strong GAL4 expression compromises *Drosophila* fat body function

Scott A. Keith [1,2,*] Ananda A. Kalukin [1,2] Dana S. Vargas Solivan,[1,2] Melanie R. Smee [1,2] Brian P. Lazzaro [1,2]

[1]Department of Entomology, Cornell University, Ithaca, NY 14853, United States
[2]Cornell Institute of Host-Microbe Interactions & Disease, Cornell University, Ithaca, NY 14853, United States

*Corresponding author: Department of Entomology, Comstock Hall, 129 Garden Ave, Cornell University, Ithaca, NY 14853, United States. Email: sk2649@cornell.edu

The ability to direct tissue-specific overexpression of transgenic proteins in genetically tractable organisms like *Drosophila melanogaster* has facilitated innumerable biological discoveries. However, transgenic proteins can themselves impact cellular and physiological processes in ways that are often ignored or poorly defined. Here we discovered that the *yolk-GAL4* transgene, which directs strong expression of the yeast GAL4 transcription factor in the *Drosophila* fat body, induces significant physiological defects in adult female flies. We found that *yolk-GAL4* disrupts adipose tissue integrity and reduces fat body lipid stores, egg production, and resistance to systemic bacterial infections. Knocking down *GAL4* expression in *yolk-GAL4* heterozygotes using RNAi fully suppressed each of these defects, thus confirming that the GAL4 transgene product induces these phenotypes. Comparing a panel of additional fat body driver lines, we found that *GAL4* expression levels directly correlate with infection susceptibility, but not with fat levels or egg production. To determine whether other transgenic proteins can impair fat body function, we constructed new fly lines in which the *yolk* enhancer directs expression of either cytoplasmic or nuclear-localized mCherry, or an alternative transactivator, LexA. We found that only nuclear-localized mCherry and LexA increased infection susceptibility similarly to GAL4, suggesting that intranuclear transgenic proteins in general can curtail the fat body's induced immune response in a manner highly sensitive to transgene expression strength. Additionally, these new lines can be valuable tools for future studies. More broadly, our findings highlight the potential for transgenes to substantially impact organismal biology and emphasize the importance of rigorously characterizing genetic tools to optimally leverage model systems like *Drosophila*.

Keywords: GAL4; *Drosophila*; fat body; adipocytes; innate immunity; metabolism; oogenesis; transgenes; nuclear import

Introduction

Cells and tissues dynamically modulate transcription, translation, metabolism, secretion, and other functions to sustain the health and fitness of multicellular organisms. Internal and external factors that disrupt the tightly coordinated balance among these processes, or that overburden any particular process, can induce cellular strain leading to tissue- and organism-level dysfunction. In some cases, the introduction of transgenes utilized to study gene expression and protein function can disrupt tissue homeostasis in genetically amenable model organisms (Liu et al. 1999; Huang et al. 2000; Detrait et al. 2002; Kramer and Staveley 2003; Krestel et al. 2004; Rezával et al. 2007; Liu and Lehmann 2008; Kintaka et al. 2016, 2020; Namba and Moriya 2024; Verma et al. 2024). These effects can complicate molecular investigations because high-level expression of the transgene is often desired to maximize the strength of experimental manipulations. However, overly strong expression and consequent high levels of the transgenic protein product may induce cellular strain that inadvertently affects the traits being studied, potentially confounding observed phenotypes and their biological significance.

The advent of the *GAL4-UAS* system marked a watershed advance for genetic experimentation in *Drosophila melanogaster*. In this bipartite expression system, *Drosophila* promoter or enhancer sequences direct expression of the *Saccharomyces cerevisiae* GAL4 transcription factor, either ubiquitously or in specific tissues and/or developmental stages. Flies expressing GAL4 under the desired regulation are then crossed to flies carrying a transgene downstream of the yeast *Upstream Activation Sequence* (*UAS*), which is a transcriptional promoter recognized by GAL4. Resultant F1 progeny bearing both genetic elements will thus express the *UAS*-linked transgene only in the cells or tissues producing GAL4 (Brand and Perrimon 1993). This system thereby enables facile, precise, and sophisticated genetic manipulations via simple experimental mating schemes. However, the potential effects of GAL4 itself on fly cell biology and physiology are rarely considered and often remain poorly defined (but see Kramer and Staveley 2003; Rezával et al. 2007; Liu and Lehmann 2008; Zappia et al. 2024).

The fat body is a tissue that governs whole-organism physiology in *Drosophila* and other insects. Composed of segmented, planar sheets of adipocytes, the fat body is distributed throughout the body segments, lining the cuticle and surrounding the visceral organs in the abdominal cavity (Johnson and Butterworth 1985). In adult flies, the fat body performs a variety of critical functions. As the primary metabolic organ, the fat body converts consumed nutrients into energy storage molecules like triglycerides and

Received on 18 July 2025; accepted on 26 October 2025

glycogen, and mobilizes these reserves as necessary to sustain the energetic needs of the animal (Canavoso et al. 2001; Arrese and Soulages 2010; Zheng et al. 2016). The fat body is also a highly secretory tissue, which releases a variety of molecules, including proteins, into the hemolymph. In female flies, the fat body produces vitellogenins, or "yolk" proteins, which are secreted and taken up by the ovary to serve as a nutrient source for developing oocytes (Isaac and Bownes 1982; Minoo and Postlethwait 1985; Bownes and Blair 1986). In response to systemic microbial infections, the fat body is one of the main immunologically active tissues, expressing and secreting high levels of microbicidal immune effector molecules, including antimicrobial peptides (AMPs; Tzou et al. 2000; Vaibhvi et al. 2022; Yu et al. 2022; Westlake et al. 2025). Because of this polyfunctionality and influence on other organ systems, the fat body plays an integral role in maintaining the overall health and physiological homeostasis of the animal. Moreover, the necessity of simultaneously carrying out multiple biological processes, often in response to dynamic extrinsic factors like dietary intake or infection, may cause the fat body to be particularly vulnerable to cellular strain.

The *yolk-GAL4* driver (also referenced as "*YP1-GAL4*") is frequently used to conduct genetic manipulations in the adult fat body. In detail, the *P{yolk-GAL4}* transgene consists of a 1,546 base pair sequence including the entire regulatory region between the vitellogenin-encoding genes *Yolk protein 1* (*Yp1*) and *Yolk protein 2* (*Yp2*), followed by *GAL4* coding sequence (Fig. 1a; https://flybase.org/reports/FBsf0000933519; Georgel et al. 2001; Vidal et al. 2001). The native *Yp1* and *Yp2* genes are primarily expressed in the fat body and follicular epithelium of vitellogenic egg chambers in adult females (Gavin and Williamson 1976; Brennan et al. 1982; Isaac and Bownes 1982; Minoo and Postlethwait 1985; Bownes and Blair 1986). Accordingly, the *yolk-GAL4* transgene is only expressed in adult females (Supplementary Fig. 1; Stronach et al. 2014), predominantly in the fat body and ovarian follicle cells (Fig. 1, b and b′, Supplementary Fig. 1a, b′, i, i′). This expression pattern affords the technical advantage of inducing UAS-activated transgene expression only in the adult stage, thereby avoiding developmental lethality or other confounding effects that might result from expression of particular transgenes in the larval fat body. The inherent adult specificity of *yolk-GAL4* obviates the need for temporal control systems that rely on inducible de-repression or activation of GAL4 protein, such as $GAL80^{TS}$ (McGuire et al. 2003), $GAL80^{AID}$ (McClure et al. 2022), and GeneSwitch (Osterwalder et al. 2001), which all require temperature or dietary treatments that can have major impacts on fly physiology (Linder et al. 2008; Yamada et al. 2017; Klepsatel et al. 2019; Robles-Murguia et al. 2019; Ma et al. 2021; Gandara and Drummond-Barbosa 2022; Fleck et al. 2024). Despite these benefits and the extensive use of *yolk-GAL4* in over 70 published studies (https://flybase.org/reports/FBtp0014828.html), a few pieces of evidence have suggested potential deleterious effects from this transgene, particularly in relation to defense against pathogen challenge. Compared to nontransgenic flies, females carrying *yolk-GAL4* have been reported to display an attenuated innate immune response to bacterial infection (Kim et al. 2014) and to sustain higher viral titers when challenged with the insect-vectored Bluetongue virus (Shaw et al. 2012). However, the potential effects of *yolk-GAL4* on immunity or other fat body-regulated processes have not been carefully examined.

Here, we show that *GAL4* expression activated by the *yolk* regulatory sequence severely compromises cellular and physiological functions of the adult *Drosophila* fat body. Our analyses reveal that high levels of *GAL4* in the fat body can disrupt lipid storage, oogenesis, and immune performance, and suggest that accumulation of various transgenic proteins in adipocyte nuclei reduces the ability of female flies to withstand bacterial infection.

Materials and methods

Drosophila stocks and husbandry

Genotypes and sources of all fly lines used in this study are detailed in Supplementary Table 1. All stock and experimental flies were cultured on a diet consisting of (weight per volume or volume per volume) 6% cornmeal, 6% yeast, 4% sucrose, 0.7% agar, 0.265% methylparaben, 0.05% phosphoric acid, and 0.5% propionic acid. Flies were maintained at 25 °C on a 12H:12H light:dark cycle. Except where indicated, all experiments were conducted with sibling-mated females aged 6 to 7 d post-eclosion.

Sequence data and information on fly stocks, transgenes, and gene function were obtained from FlyBase (release FB2025_02) (Jenkins et al. 2022).

Tissue staining and fluorescence imaging

To visualize the expression patterns of fat body *GAL4* lines and *yolk-LexA* flies, males of the indicated driver genotype were crossed to virgin females carrying either *UAS-mCD8::GFP* or *LexAop-mCD8::GFP* to generate F1 progeny heterozygous for both the driver and responder elements. Expression patterns of the *yolk-mCherry.cyt* and *yolk-mCherry.nls* transgenes were visualized in tissues from flies homozygous for each transgene. Adult females were aged 6 to 7 d post-eclosion at 25 °C (or 29 °C for *3.1Lsp2 > mCD8::GFP* flies; Supplementary Fig. 4ba–bf) and dissected in ice-cold PBS (pH 7.4; Sigma) to isolate the brain, thoracic flight muscle, ovaries, gut, Malpighian tubules, and abdominal carcass. Larval fat bodies were dissected at the late third instar stage, ~96 h post egg-laying. Tissues were fixed in 4% paraformaldehyde-PBS (Electron Microscopy Sciences) for 30 min, washed 3 times in PBS 0.3% Triton X-100 (PBT), and stained with DAPI (1 µg/mL in PBS; Invitrogen) for 15 min at room temperature to label cell nuclei. Tissues were washed in PBS and mounted in ProLong Glass Antifade Mountant (Invitrogen).

Epifluorescence images were acquired on a Leica DM5000B upright microscope with a CTR5000 controller, EL6000 light source, and DFC365 FX camera using LAS AF 2.6 software. All images of driver-induced GFP expression (Fig. 1, b and b′; Fig. 7b–c′; Supplementary Figs. 1 and 4) or mCherry fluorescence (Fig. 6a–d; Supplementary Fig. 7) were acquired with identical imaging settings.

Oil red O staining and image analysis

Abdominal fat tissue was visualized by Oil Red O staining following established protocols (Gutierrez et al. 2007; Molaei et al. 2019). Dissected abdominal carcasses were fixed as described above and stained for 30 min in freshly prepared Oil Red O solution: 6 mL 0.1% Oil Red O (Sigma) dissolved in isopropanol and 4 mL distilled water passed through a 0.22 µm filter. Carcasses were rinsed 3 times with distilled water, mounted as described above, and imaged on a Leica M165 FluoCombi stereomicroscope system.

Oil Red O staining intensities were quantified using FIJI. Color images were converted to 8-bit pixel depth and inverted. For each carcass, a constant 477 × 525 pixel region of interest was positioned over abdominal segments A2-A5 (Yoder 2012; Jürgens et al. 2024) and mean pixel intensity was measured within this area.

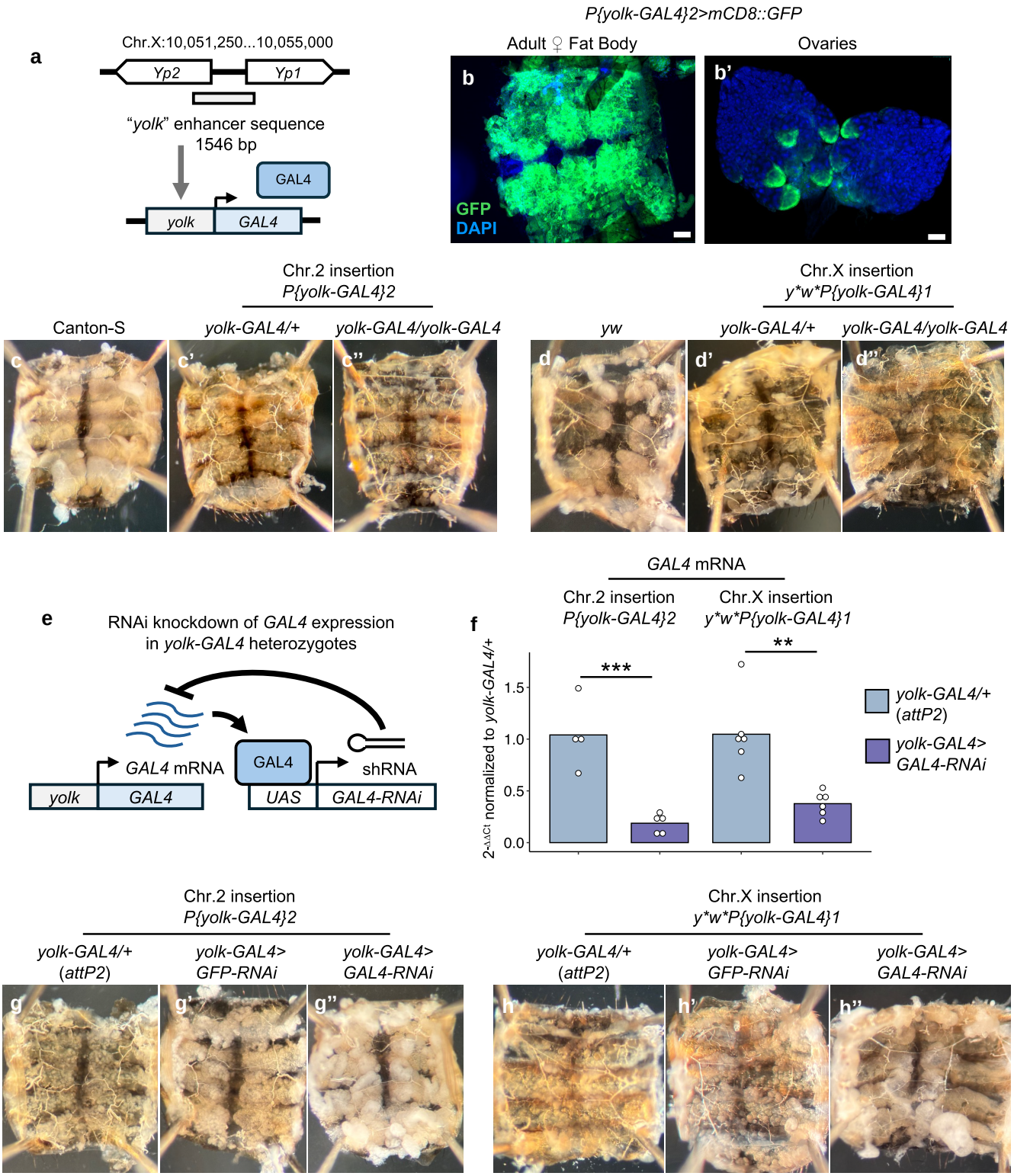

Fig. 1. *GAL4* expression under control of the *yolk* regulatory sequence disrupts tissue integrity of the adult fat body. a) Schematic illustrating design of the *yolk-GAL4* transgene (Vidal et al. 2001). Regulatory sequence spanning the intergenic region between the yolk protein-encoding genes *Yp1* and *Yp2* directs expression of the *S. cerevisiae* GAL4 transcription factor. (b,b′) Expression pattern of a *UAS-mCD8::GFP* reporter induced by *yolk-GAL4* indicates GAL4 expression in the adult female fat body (b) and follicle cells of maturing oocytes in the ovary (b′). Nuclei are stained with DAPI to delineate overall tissue morphology. Scale bars = 100 µm. (c-d″) Abdominal filets dissected from 6 to 7 d old adult females displaying fat body tissue lining the internal surface of the dorsal cuticle. Females heterozygous or homozygous for the same *yolk-GAL4* transgene integrated on either the second chromosome (c′, c″) or the X chromosome (d′, d″) contain thin, fragmented fat bodies, compared to robust adipose tissue in abdomens of nontransgenic Canton-S (c) and *yw* (d) control females. e) Schematic illustrating genetic approach to reduce GAL4 expression levels in *yolk-GAL4* females. GAL4 protein produced from the *yolk-GAL4* transgene activates expression of a separate *UAS*-controlled transgene, which produces an RNA hairpin construct complementary to *GAL4* transcript

(continued)

Starvation survival analysis

Flies were transferred to 1% (weight per volume) agarose-water vials and maintained at 25 °C on a 12H:12H light:dark cycle. Mortality was scored 3 times per day until the entire population succumbed.

Egg laying and hatch rate assays

For egg laying assays, females were collected as virgins 0 to 4 h post-eclosion and placed in food vials with the above-described diet in groups of 2 or 3 flies per vial with an equal number of Canton-S males. Flies were flipped to new food vials every 24 h. Total eggs laid in each 24 h time period were counted and divided by the number of females in the vial to approximate the number of eggs laid per fly. These daily values were summed to calculate total eggs laid per fly over the 7 d experimental period.

To assay embryo viability, the numbers of eggs laid in food vials over a 24 h period were counted and resulting progeny were allowed to develop to the pupal stage for 8 d 25 °C. Hatch rates were calculated as the ratio of the number of pupae to the number of eggs laid in each vial.

Ovary size and egg chamber stage analyses

For all genotypes analyzed, ovaries were dissected from females co-housed with males in groups of 10 to 15 flies per vial (containing the above-described diet) and aged 7 d post-eclosion. To control for dietary impacts on oogenesis, flies were transferred to fresh food vials every other day so nutrient availability to adults would not be impacted by the presence of larvae. Whole intact ovaries were dissected in PBS and immediately imaged on a Leica M165 FluoCombi stereomicroscope system. Ovary size was quantified in FIJI, using the polygon selection tool to trace the outline of each ovary image and measure the area within the outlined region.

Numbers of vitellogenic follicles, mature oocytes, and ovarioles per ovary were counted by visual inspection of dissected ovaries under a stereomicroscope. Vitellogenic follicles (stages 8 to 13) were identified by the presence of opaque, yolk-filled oocytes morphologically distinguishable from nurse cells (Jia et al. 2016). Mature, stage 14 oocytes were identified by the presence of fully formed dorsal appendages (Bastock and St Johnston 2008).

Bacterial infection procedures and infection survival analysis

Flies were systemically infected with *Providencia rettgeri* strain Dmel (Juneja and Lazzaro 2009), *Enterococcus faecalis* Dmel (Lazzaro 2002) or *Pectobacterium carotovorum* (formerly known as *Erwinia carotovorum*, *Ecc15*; Basset et al. 2000) following procedures described in Khalil et al. (2015). Flies were briefly anesthetized on CO_2 platforms and *P. rettgeri* and *E. faecalis* infections were administered by dipping a 0.15 mm minutien pin in the bacterial inoculum and pricking flies in the sternopleural region of the thorax. *Ecc15* infections were administered by injecting 23 nL of bacterial suspension into the thorax with a Drummond Nanoject II nanoinjector. Bacterial cultures were grown overnight in either Luria–Bertani (LB) broth (*P. rettgeri* and *Ecc15*) or brain heart infusion (BHI) broth (*E. faecalis*). *P. rettgeri* cultures were grown at 37 °C with shaking, and *E. faecalis* and *Ecc15* cultures were grown at 30 °C with shaking. Overnight cultures were pelleted by centrifugation and resuspended in sterile phosphate-buffered saline (PBS). *P. rettgeri* and *E. faecalis* inocula were standardized to optical density (OD_{600}) = 1, corresponding to ~300 colony forming units (CFU) per pinprick, while *Ecc15* was standardized to OD_{600} = 10, corresponding to ~10^5 CFU injected into each fly. To quantify bacterial doses administered with each infection, 4 to 8 flies were infected and immediately homogenized and plated to enumerate CFUs as described below.

Infected flies were housed in food vials in groups of 10 to 15 individuals per vial at 25 °C and flipped to fresh vials every other day due to the growth of larval progeny in the food substrate. To quantify infection-induced mortality, the number of dead flies in each vial was counted daily for 5 d post-infection.

Bacterial load analysis

Individual flies were collected at the indicated timepoints post-infection and homogenized in 250 µL PBS with 2.3 mm chrome steel disruption beads (Research Products International) via bead-beating for 30 s with a Mini-BeadBeater-96 tissue disrupter (BioSpec Products). Homogenates were diluted 1:10 and 1:100 in PBS, and each dilution was plated on LB agar with a Whitley Automated Spiral Plater 2 (Don Whitley Scientific). Plates were incubated at 37 °C overnight and resulting colonies were counted from dilution plates that yielded distinct, individual colonies using a ProtoCOL3 plate counter (Microbiology International). CFU per mL values obtained from the ProtoCOL3 software were used to calculate the number of viable bacterial cells in each fly with the following equation: CFU/fly = (CFU/mL) × (dilution factor) × (0.25 mL).

RT-qPCR and RT-PCR

Whole flies or dissected tissues were homogenized for 30 s in 500 µL Trizol reagent (Invitrogen) with 2.3 mm zirconia/silica beads (BioSpec Products) via bead-beating. Total RNA was extracted using the Zymo Research Direct-zol RNA miniprep kit and cDNA was synthesized from 500 ng RNA template with Bio-Rad iScript Reverse Transcription Supermix. qPCR was performed with PerfeCTa SYBR Green FastMix (Quantabio) on a Bio-Rad CFX Connect thermocycler. Expression levels for genes of interest were calculated as $\Delta\Delta C_t$ values:

1) For each sample, C_t values of the housekeeping gene *Rpl32* were subtracted from C_t values of the gene of interest: $\Delta C_{tGOI} = C_{tGOI} - C_{tRpl32}$
2) Experimental genotypes/conditions were normalized to control genotypes/conditions by first averaging the ΔC_t values for the control group and then subtracting this average value from the ΔC_t values of each individual experimental sample: $\Delta\Delta C_{tGOI} = \Delta C_{texperimental\_sample} - \text{average}(\Delta C_{tcontrol\_samples})$

Fig. 1. (Continued)
sequence, thus leading to RNAi-mediated suppression of *GAL4* expression. f) RT-qPCR analysis indicates that expressing the *UAS-GAL4-RNAi* construct substantially reduces *GAL4* expression levels in *yolk-GAL4* heterozygous females. Data represent $2^{-\Delta\Delta Ct}$ values normalized to the mean ΔC_t value for control females with *yolk-GAL4* heterozygous over the *attP2* genetic background. Each dot represents an individual sample of 5 to 10 pooled flies, bars represent the mean. $^{**}P < 0.01$, $^{***}P < 0.001$, unpaired two-sample *t*-test. (g-h″) Females carrying *yolk-GAL4* heterozygous over the *attP2* genetic background (g, h), or expressing a *UAS-GFP-RNAi* construct (to control for nonspecific effects of RNAi activation; g′, h′) contain fat bodies with morphological defects comparable to heterozygotes in (c′, d′). Knocking down *GAL4* expression fully suppresses the aberrant fat body morphology caused by either the second chromosome (g″) or X chromosome (h″) *yolk-GAL4* insertion, indicating these phenotypes are caused by GAL4.

For RT-PCR confirmation of *UAS-p35* transgene expression (Supplementary Fig. 6a), RNA was extracted and cDNA synthesized as described above. PCR amplification was conducted from cDNA template using GoTaq Green Master Mix (Promega) and the following cycling conditions: 2 min initial denaturation at 95 °C, followed by 30 cycles of 30 s denaturation at 95 °C, 30 s annealing at 50 °C, and 1 min elongation at 72 °C. Reaction products were resolved on a 1.5% agarose gel with SYBR Safe DNA gel stain (Invitrogen).

Primer sequences are listed in Supplementary Table 2.

Generation of *yolk-mCherry.cyt* and *yolk-mCherry.nls* lines

pYolk-mCherry.NLS-attB and *pYolk-mCherry.CYT-attB* plasmids were generated by VectorBuilder Inc. The *yolk* regulatory sequence used for construction of the *yolk-GAL4* transgene (https://flybase.org/reports/FBsf0000933519) was cloned upstream of *mCherry* coding sequence, replacing the *UASt-Hsp70p* regulatory sequence in the *pUASt.attB* vector backbone. In the *pYolk-mCherry.NLS-attB* construct, *mCherry* is flanked by 5′ and 3′ nuclear localization signal sequences. Constructs were injected into *M{vas-int.Dm}ZH-2A; P{CaryP}attP40* embryos by BestGene, Inc. for ΦC31-mediated transgene integration at the second chromosome *attP40* docking site. Positive transformants were selected by expression of a *mini-white* eye marker, balanced, and established as stable lines in a w^{1118} background.

Generation of *yolk-LexA* by HACKy-mediated conversion of *yolk-GAL4*

The second chromosome *yolk-GAL4* insertion was converted to *yolk-LexA* following the "version 2" HACKy approach detailed in Rankin et al. (2024). The crossing scheme employed for conversion is presented in Supplementary Fig. 9a. First, *yolk-GAL4* males (expressing a *mini-white*$^+$ visible marker) were crossed to females carrying a germline-expressed *vas-Cas9* transgene and the HACKy donor cassette (abbreviated "*CyO, PBac{LexA.G4H, RFP*$^+$*, y*$^+$*}*"). The HACKy donor comprises: (i) U6 promoter-expressed guide RNAs targeting the *GAL4* coding sequence, (ii) the *LexA::GAD* coding sequence flanked by *GAL4* homology arms and separated from the 5′ homology arm by T2A ribosomal skipping sequence, and (iii) the *3xP3-RFP* and $y^{+t7.7}$ visible markers. Eighty individual F1 males, carrying *vas-Cas9* on the X chromosome and *yolk-GAL4* in trans to *CyO, PBac{LexA.G4H, RFP*$^+$*, y*$^+$*}* were mated to 2 to 3 y^1w^{67c23}; sna^{ScO}/*CyO* virgin females each. We screened ~50 to 100 F2 progeny from each F1 cross and identified a single, balanced male expressing all 3 *mini-white*$^+$, *y*$^+$, and *3xP3-RFP* markers, indicative of successful conversion. This male was sequentially crossed to y^1w^{67c23}; sna^{ScO}/*CyO* virgin females to establish a stable line, and then to *LexAop-mCD8::GFP* virgin females to confirm GFP expression in the spatiotemporal pattern matching that activated by *yolk-GAL4*.

Statistical analyses

All statistical tests were performed with R version 4.4.0 (https://R-project.org). For all experiments except survival analyses, data normality was first evaluated by Shapiro–Wilk test and homogeneity of variance assessed by Levene's test. Data that met parametric test assumptions (normal distribution and equal variance among groups) were analyzed by unpaired, two-sample *t*-test (2 experimental genotypes), or by one-way ANOVA with Tukey's post hoc comparisons (3 or more genotypes). Data that did not meet parametric test assumptions were compared via Mann–Whitney test or Kruskal–Wallis test with Dunn's post hoc comparison. Figure legends indicate the test used for each experiment. Infection and starvation survival data were analyzed via pairwise Log-Rank test with Benjamini–Hochberg correction using the pairwise_survdiff() function in the survminer package (Kassambara et al. 2024). The significance threshold was considered $P < 0.05$. Sample sizes for each dataset are reported in Supplementary Table 3.

Results

GAL4 expression under control of the *yolk* regulatory sequence disrupts tissue morphology of the adult female fat body

The *yolk-GAL4* transgene directs GAL4 expression specifically in the adult female fat body (Fig. 1b, Supplementary Fig. 1a, a′, i, i′) and in the follicle cells of late-stage oocytes (Fig. 1b′, Supplementary Fig. 1b, b′) with additional activity observed in the crop duct (Supplementary Fig. 1e, e′, j, j′). While attempting to conduct genetic manipulations with a fly line carrying *yolk-GAL4* integrated on the second chromosome (*P{yolk-GAL4}2*), we noticed that the adipose tissue of flies harboring this construct exhibited striking morphological defects. Fat bodies lining the dorsal abdomen of *P{yolk-GAL4}2* heterozygotes appeared thin, fragmented, and clumpy (Fig. 1c′) compared to the robust sheets of adipose tissue in wild-type Canton-S flies (Fig. 1c). We observed comparable aberrant tissue integrity in fat bodies of *P{yolk-GAL4}2* homozygous females (Fig. 1c″).

These observations suggested that *GAL4* expressed under the control of the *yolk* promoter could disrupt fat body tissue integrity. However, the *P{yolk-GAL4}2* line was generated by P-element-mediated integration at an unmapped genetic locus on the second chromosome (Georgel et al. 2001; Vidal et al. 2001). Thus, in principle, the *yolk-GAL4* insertion might disrupt the expression or function of a gene necessary to maintain fat body tissue integrity. To address this possibility, we examined a separate fly line carrying the same *P{yolk-GAL4}* construct integrated on the X chromosome (*P{yolk-GAL4}1*), and therefore at an entirely different genomic locus. Females carrying 1 or 2 copies of *P{yolk-GAL4}1* contained fragmented fat bodies morphologically similar to those observed in *P{yolk-GAL4}2* females (Fig. 1, d′ and d″). These results strongly suggest that the aberrant fat body morphology of *yolk-GAL4* flies is caused by expression of the transgene, and not by inadvertent insertional mutagenesis of an unidentified gene.

We reasoned that if the aberrant fat body morphology we observed in *yolk-GAL4* females were truly caused by GAL4, then blocking *GAL4* expression should alleviate this defect. To test this prediction, we generated *yolk-GAL4* heterozygotes with self-targeted, RNAi-mediated inhibition of *GAL4* expression (Fig. 1e). Specifically, we crossed each of the 2 *yolk-GAL4* insertion lines to flies carrying a *UAS*-activated RNA hairpin construct targeting the *GAL4* coding sequence. Expression of GAL4 protein, therefore, results in RNAi knockdown of the *GAL4* transgene in F1 progeny (Fig. 1e). For controls, we crossed *yolk-GAL4* flies with the genetic background line in which the *UAS-GAL4-RNAi* stock was generated ("*attP2*"), and with flies carrying a *UAS-GFP-RNAi* construct to control for nonspecific effects of RNAi activation. RT-qPCR analysis confirmed that *GAL4* mRNA levels were substantially reduced when *GAL4* RNAi was activated by either *P{yolk-GAL4}2* or *P{yolk-GAL4}1* (Fig. 1f).

We found that *GAL4* knockdown fully suppressed the aberrant fat body morphology caused by heterozygosity for *yolk-GAL4*. Females carrying either *yolk-GAL4* insertion heterozygous over the *attP2* background, or with *yolk-GAL4* activating expression of

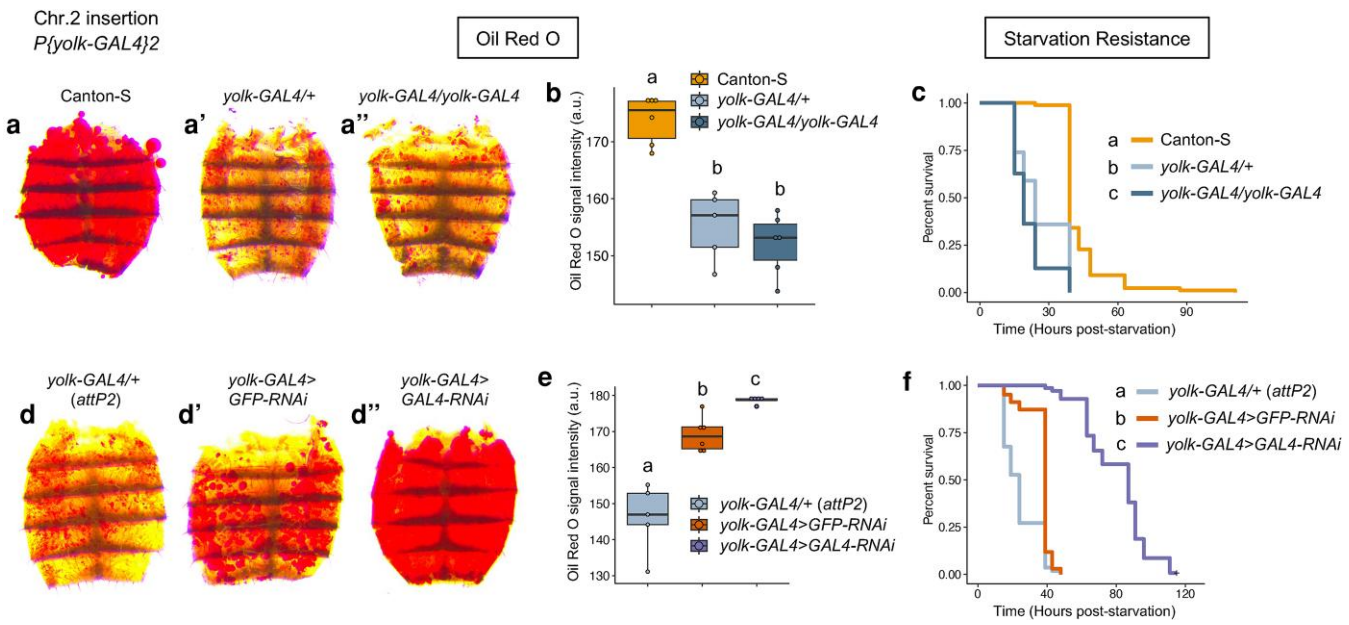

Fig. 2. Expression of *yolk-GAL4* reduces fat body lipid stores and increases starvation sensitivity. (a-a″) Representative images of abdominal filets dissected from 6 to 7 d old adult females of the indicated genotypes, stained with the lipophilic dye Oil Red O (ORO). Females heterozygous (a′) or homozygous (a″) for the second chromosome *yolk-GAL4* insertion display weaker abdominal ORO staining compared to nontransgenic Canton-S controls (a). b) Quantification and statistical comparisons of ORO staining intensities. c) Females carrying *yolk-GAL4* succumb to starvation faster than nontransgenic control females. (d-f) Knocking down *GAL4* expression by using *yolk-GAL4* to induce *GAL4*-targeting RNAi (see Fig. 1, e and f) increases abdominal fat levels (d-d″, e) and extends starvation survival time (f) in females carrying *yolk-GAL4*. For ORO signal intensity data (b,e) each dot represents an individual abdomen/fly, a.u.=arbitrary units. Statistics: ORO data were analyzed by one-way ANOVA with Tukey's post-hoc pairwise comparisons (b,e). Starvation survival data were analyzed by pairwise Log-Rank tests with Benjamini–Hochberg correction for multiple comparisons (c,f). Genotypes with different letters are statistically different from one another ($P < 0.05$). All sample sizes are reported in Supplementary Table 3.

the *UAS-GFP-RNAi* construct, contained thin, clumpy fat bodies similar to those observed with *yolk-GAL4* in *trans* to Canton-S or *yw* backgrounds (Fig. 1, g and g′, h, h′). By contrast, females heterozygous for *yolk-GAL4* with RNAi-mediated *GAL4* knockdown displayed robust, contiguous fat body sheets comparable to those observed in flies lacking the transgene (Fig. 1, g″ and h″). Taken together, these results indicate that *GAL4* expression activated by the *yolk* regulatory sequence compromises the gross-level tissue integrity of the adult fat body.

yolk-GAL4 expression impairs major physiological functions of the adult fat body

Having found that *yolk-GAL4* compromises adipose tissue integrity, we hypothesized that expression of this transgene might also impact major physiological processes regulated by the adult female fat body, namely energy storage, immunity, and reproduction.

yolk-GAL4 *expression reduces lipid stores and starvation resistance*

Females heterozygous or homozygous for *yolk-GAL4* contained thin, fragmented fat body tissue (Fig. 1, c′ and c″, d′, d″, g, g′, h, h′). We therefore asked whether this degenerated tissue appearance might be accompanied by reduced levels of stored lipids. To answer this question, we visualized gross fat levels in wild-type, *yolk-GAL4/+* and *yolk-GAL4/yolk-GAL4* females by staining dissected abdominal carcasses with the lipophilic dye Oil Red O (ORO). ORO nonspecifically labels neutral lipids, including triglycerides (Ramírez-Zacarías et al. 1992), which constitute the primary class of lipids in the *Drosophila* fat body (Canavoso et al. 2001; Parisi et al. 2011; Kühnlein 2012). We found that 1 or 2 copies of either *P{yolk-GAL4}2* (Fig. 2, a′ and a″) or *P{yolk-GAL4}1* (Supplementary Fig. 2a′, a″) resulted in significantly weaker ORO staining intensity compared to Canton-S (Fig. 2a) or *yw* (Supplementary Fig. 2a) controls (Fig. 2b, Supplementary Fig. 2b). Reduced fat levels are frequently accompanied by greater sensitivity to full nutrient deprivation (Da Lage et al. 1989; Zwaan et al. 1991; Chippindale et al. 1996; Gibbs and Reynolds 2012; Chauhan et al. 2021). Consistent with their reduced abdominal lipid content, we found that females carrying *yolk-GAL4* succumbed to starvation considerably more rapidly than nontransgenic controls (Fig. 2c, Supplementary Fig. 2c). Notably, for both *yolk-GAL4* insertion lines, heterozygotes survived moderately but significantly longer than homozygotes (Fig. 2c, Supplementary Fig. 2c), suggesting a dose-dependent effect of *GAL4* on starvation sensitivity.

To confirm that GAL4 caused the low fat content and starvation sensitivity of *yolk-GAL4* flies, we again reduced *GAL4* expression levels by RNAi and quantified ORO staining and starvation resistance. We found that knocking down *GAL4* expression from either *P{yolk-GAL4}2* or *P{yolk-GAL4}1* led to higher fat levels (Fig. 2d″, Supplementary Fig. 2d″) and increased starvation resistance (Fig. 2f, Supplementary Fig. 2f) compared to control animals with *yolk-GAL4* heterozygous over the *attP2* background (Fig. 2, d and e, Supplementary Fig. 2d, e) or with *yolk-GAL4* activating expression of the *UAS-GFP-RNAi* construct (Fig. 2, d′ and e, Supplementary Fig. 2d′, e). Of note, for both insertions, *yolk-GAL4 > GFP-RNAi* females displayed less severe fat depletion and starvation sensitivity than *yolk-GAL4/attP2* females (Fig. 2, d and d′, e, f, Supplementary Fig. 2d, d′, e, f). This could be due to the *UAS-GFP-RNAi* line harboring genetic background elements that partially suppress these phenotypes. Alternatively, these data might indicate that GAL4-induced tissue dysfunction can be partially attenuated solely by binding *UAS* sites or by non-specific induction of RNAi mechanisms.

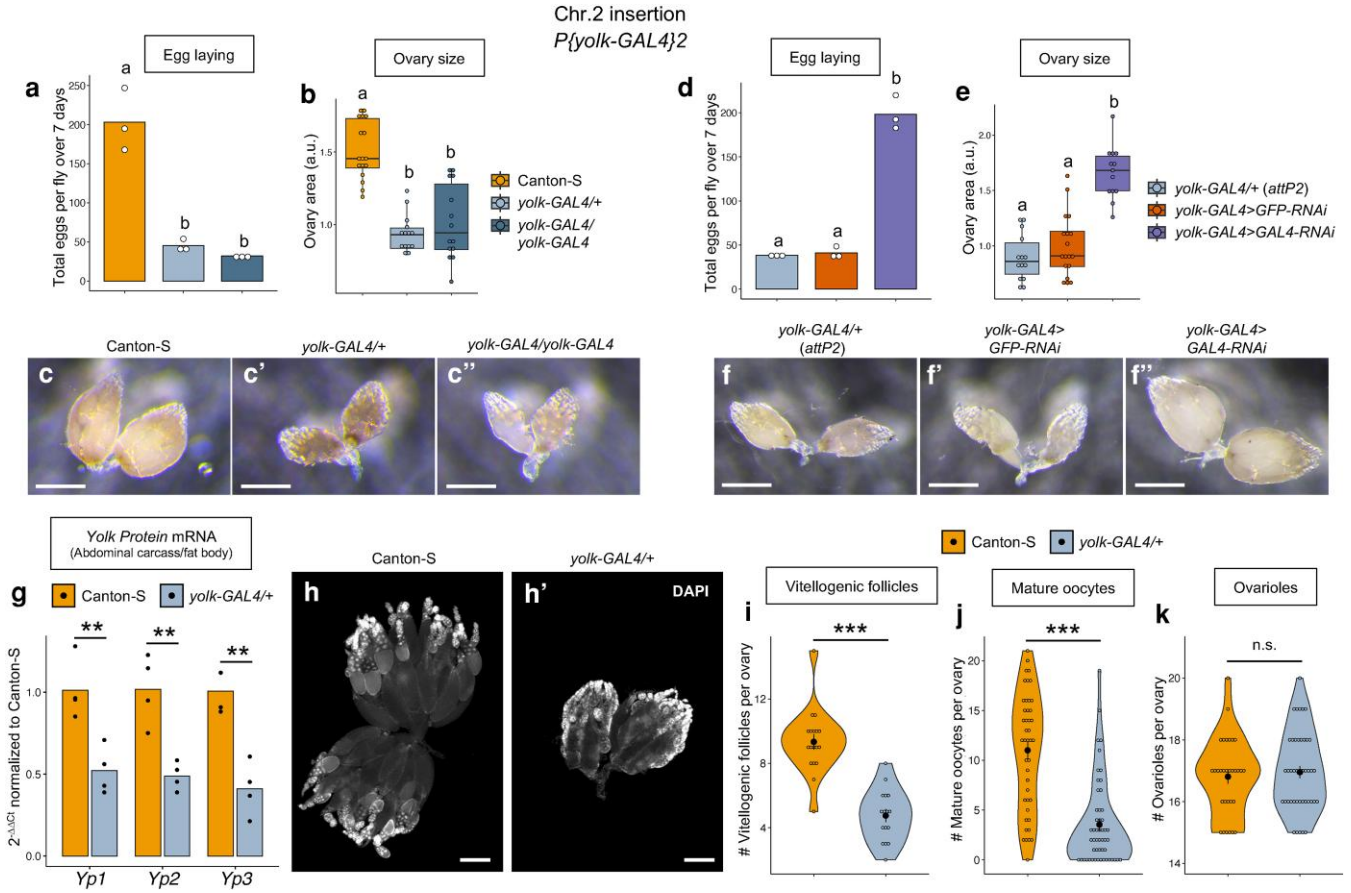

Fig. 3. Females expressing *yolk-GAL4* exhibit oogenesis and egg laying defects. a) Females heterozygous or homozygous for *yolk-GAL4* lay dramatically fewer eggs compared to nontransgenic Canton-S females. (b-c″) Ovaries from females carrying 1 or 2 copies of *yolk-GAL4* are stunted in size compared to ovaries from wild-type, Canton-S females. Representative images of whole dissected ovaries are presented in (c-c″). (d-f″) Reducing *GAL4* expression by RNAi fully suppresses the egg laying deficit (d) and ovary stunting (e-f″) caused by heterozygosity for *yolk-GAL4*. For egg laying data (a,d), each point represents an individual replicate, 2 to 3 females per replicate, bars represent the mean. For quantification of ovary size (b,e), each point represents an individual ovary. Box plots represent the median, first and third quartiles, and 1.5 × interquartile range, a.u.=arbitrary units. Scale bars = 500 µm. g) RT-qPCR analysis shows that expression of the 3 major Yolk Protein-encoding genes is reduced in fat bodies of females heterozygous for *yolk-GAL4*. Data represent $2^{-\Delta\Delta Ct}$ values normalized to the mean ΔC_t value for Canton-S samples. Each dot represents an individual sample of 10 pooled fat bodies/abdominal carcasses, bars represent the mean. (h,h′) Ovaries dissected from nontransgenic Canton-S females (h) and *yolk-GAL4* heterozygous females (h′) with DAPI-stained nuclei to reveal developmental stages of individual egg chambers. Scale bars = 100 µm. (i-k) Ovaries from *yolk-GAL4* heterozygotes contain fewer vitellogenic egg chambers (i) and fewer mature oocytes (j) than ovaries from wild-type females, while total numbers of ovarioles per ovary do not differ (k). For violin plots, each point represents counts from an individual ovary. Opaque point represents the mean and bars represent standard error. Statistics: Egg laying data (a,d) were analyzed by one way ANOVA with Tukey's post hoc pairwise comparisons. Ovary size data were analyzed by Kruskal–Wallis test with Dunn's post hoc pairwise comparisons (b) or by one way ANOVA with Tukey's post hoc pairwise comparisons (e). Genotypes with different letters are statistically different from one another ($P < 0.05$). RT-qPCR data (g) and vitellogenic egg chamber counts (i) were analyzed by unpaired two-sample *t*-test. Mature oocyte counts (j) were analyzed by Mann–Whitney test. $^{**}P < 0.01$, $^{***}P < 0.001$.

Collectively, these data show that expression of the *yolk-GAL4* transgene results in diminished abdominal fat stores and increased sensitivity to starvation, both indicative of disrupted metabolic homeostasis.

yolk-GAL4 *impairs oogenesis and egg laying*

yolk-GAL4 is expressed in the fat body and ovarian follicle cells (Fig. 1, b and b′, Supplementary Fig. 1a, b, i), both of which regulate oogenesis (Brennan et al. 1982; Isaac and Bownes 1982; Arrese and Soulages 2010). We therefore asked whether *yolk-GAL4* might affect egg production. To answer this question, we counted the total number of eggs laid by control females and females carrying *P{yolk-GAL4}2* for 7 d post-eclosion. This analysis revealed major egg-laying deficits caused by the *P{yolk-GAL4}2* transgene. Over the first week of adulthood, *P{yolk-GAL4}2* heterozygous or homozygous females laid on average fewer than 50 eggs, in contrast to the ~200 eggs laid by Canton-S wild-type flies (Fig. 3a). Reduced egg laying could result from decreased oogenesis or from retention of mature oocytes and reduced ovulation. Visual inspection of ovaries dissected from *P{yolk-GAL4}2* heterozygous (Fig. 3, b and c′) and homozygous (Fig. 3, b and c″) females revealed them to be dramatically stunted in size compared to the fully developed ovaries of Canton-S flies (Fig. 3, b and c), suggesting that the low egg output of *P{yolk-GAL4}2* females likely reflects oogenesis defects as opposed to reduced ovulation.

To test whether *GAL4* expression from the *yolk* enhancer leads to reduced egg laying and stunted ovaries, we again examined the X chromosome *P{yolk-GAL4}1* line and knocked down *GAL4* expression by RNAi. While *P{yolk-GAL4}1* homozygotes laid significantly fewer eggs than nontransgenic controls, heterozygosity for *P{yolk-GAL4}1* did not affect egg output (Supplementary Fig. 3a). Of note, however, *yw* females used as the control genotype for this experiment laid substantially fewer eggs than the Canton-S females used as controls for *P{yolk-GAL4}2* (compare orange bars,

Fig. 3a and Supplementary Fig. 3a). Despite these different egg laying rates, both *P{yolk-GAL4}1* heterozygotes and homozygotes contained significantly smaller ovaries than *yw* flies (Supplementary Fig. 3b–c″). Moreover, we found that knocking down *GAL4* levels fully suppressed the low egg output and reduced ovary size of females heterozygous for *P{yolk-GAL4}2* (Fig. 3d–f″) or *P{yolk-GAL4}1* (Supplementary Fig. 3d–f″), confirming that expression of the *yolk-GAL4* transgene leads to decreased egg production.

Across multiple genotypes, we noticed that females heterozygous for *P{yolk-GAL4}2* laid fewer eggs than those heterozygous for *P{yolk-GAL4}1* (compare corresponding colors between Fig. 3, a and d and Supplementary Fig. 3a, d). We speculated that this difference in phenotype severity could reflect differences in *GAL4* expression strength or pattern resulting from the distinct chromosomal insertion sites of the transgene between these 2 lines. Consistent with this, while both insertions drove robust expression of a *UAS-GFP* reporter in the fat body and crop duct (Supplementary Fig. 1a, e, i, j), we found that only *P{yolk-GAL4}2* activated visible GFP expression in the ovary (Supplementary Figs. 1b, b′, k, k′ and 3g–h′). RT-qPCR analysis confirmed that *GAL4* expression was significantly lower in ovaries of *P{yolk-GAL4}1* heterozygotes compared to *P{yolk-GAL4}2* heterozygotes (Supplementary Fig. 3i). These data suggest that the quantitative level of *GAL4* expression in the follicular epithelium might contribute to the severity of egg laying defects caused by *P{yolk-GAL4}2*.

We next asked whether ovary stunting and reduced egg laying induced by *GAL4* expression might reflect vitellogenesis defects originating from impaired yolk protein synthesis by the fat body. To test this hypothesis, we used RT-qPCR to measure *Yp1*, *Yp2*, and *Yp3* expression levels in fat bodies dissected from Canton-S and *P{yolk-GAL4}2/+* females. We found that expression of all 3 *yolk* genes was significantly reduced in females carrying *P{yolk-GAL4}2* (Fig. 3g), suggesting the transgene might curtail the fat body's ability to provide vitellogenins to developing oocytes. Closer inspection of dissected ovaries revealed that ovarioles from *P{yolk-GAL4}2/+* females contained substantially fewer vitellogenic follicles (Fig. 3, h and h′, i) and fewer mature oocytes (Fig. 3, h and h′, j) than ovaries from Canton-S females, despite the genotypes having comparable numbers of ovarioles (Fig. 3k). These data suggest that impaired yolk provisioning and consequent oogenesis failure might contribute to the low numbers of later-stage oocytes in *P{yolk-GAL4}2/+* females. Notably, >94% of the eggs laid by *P{yolk-GAL4}2* heterozygous or homozygous females yielded viable progeny, suggesting no major decline in the quality of the few oocytes that are successfully produced (Supplementary Fig. 3j).

Altogether, these findings suggest that expression of the *yolk-GAL4* transgene disrupts vitellogenesis, leading to substantially curtailed egg production.

yolk-GAL4 *compromises resistance to systemic bacterial infections*

A previous study by Kim et al. (2014) reported abrogated transcriptional upregulation of genes encoding antimicrobial peptides following *Escherichia coli* infection in *yolk-GAL4* heterozygotes compared to nontransgenic w^{1118} flies. Based on this prior study, and because the fat body is the principal tissue responsible for AMP production during systemic microbial infections (Tzou et al. 2000; Arrese and Soulages 2010; Westlake et al. 2025), we hypothesized that *yolk-GAL4* might affect immune function and infection resistance. To test this prediction, we first systemically challenged flies carrying *yolk-GAL4* with the Gram-negative bacterial pathogen *Providencia rettgeri* (Juneja and Lazzaro 2009) and monitored population survival over 5 d post-infection. Strikingly, we found that females carrying *P{yolk-GAL4}2* were extremely sensitive to *P. rettgeri*. While only ∼50% of nontransgenic Canton-S flies died over the course of 5 d, the entire population of *P{yolk-GAL4}2* heterozygotes and homozygotes succumbed primarily within 24 h and no later than 48 h after administering *P. rettgeri* (Fig. 4a). To determine whether *yolk-GAL4* females are particularly sensitive to *P. rettgeri* or whether the transgene increases susceptibility to bacterial infections in general, we also infected *yolk-GAL4*-expressing flies with the Gram-positive pathogen *Enterococcus faecalis* (Lazzaro 2002) and with the Gram-negative bacterium *Pectinobacter* (*Erwinia*) *carotovora* (*Ecc15*; Basset et al. 2000), which has relatively low virulence to wild-type flies (Troha et al. 2018). Similar to *P. rettgeri* infection, we found that >97% of *yolk-GAL4*-expressing females succumbed to *E. faecalis* infection within 48 h (Fig. 4b). Approximately 75% of females homozygous for *P{yolk-GAL4}2* succumbed to *Ecc15* infection, whereas Canton-S flies experienced ∼10% population mortality (Fig. 4c). We also observed a notable transgene dose effect. Although mortality levels for *P{yolk-GAL4}2/+* and *P{yolk-GAL4}2/P{yolk-GAL4}2* females infected with *E. faecalis* were comparable by 5 d post-infection, homozygotes succumbed more rapidly than heterozygotes (Fig. 4b). The lesser virulence of *Ecc15* revealed a particularly striking effect of transgene copy number: ∼75% of *P{yolk-GAL4}2* homozygous females succumbed to *Ecc15* infection, in contrast to the ∼34% mortality of *P{yolk-GAL4}2* heterozygotes (Fig. 4c). Importantly, 100% of heterozygous and homozygous *yolk-GAL4* females survived septic injury with sterile PBS ($n = 51$ to 89 flies per genotype), indicating that the thoracic wounding procedure alone does not contribute to the infection sensitivity of *yolk-GAL4* flies.

We conducted several additional experiments to confirm that infection susceptibility is caused by *GAL4* expression and not by confounding effects of the transgene insertion. First, we confirmed that X-chromosome-inserted *P{yolk-GAL4}1* heterozygotes and homozygotes also exhibited complete population mortality within 24 to 48 h post-infection with *P. rettgeri* (Fig. 4d), matching the mortality observed in *P{yolk-GAL4}2* females. Next, we infected *P{yolk-GAL4}1* and *P{yolk-GAL4}2* males, reasoning that these flies are genetically identical to females (excepting X/Y chromosome copy number) but they do not express the transgene due to the sex-specific activity of the *yolk* enhancer (Supplementary Fig. 1h, h′). In contrast to their female siblings, males of both genotypes survived *P. rettgeri* infection comparably to nontransgenic wild-type males (Fig. 4, e and f). Lastly, we knocked down *GAL4* expression in *yolk-GAL4* heterozygotes by RNAi. *GAL4* knockdown fully suppressed the infection susceptibility caused by *P{yolk-GAL4}2* (Fig. 4g) and *P{yolk-GAL4}1* (Fig. 4h). In summary, these data show that *yolk-GAL4* expression renders flies less able to survive systemic infections.

We next asked whether the infection susceptibility of *yolk-GAL4* females is indicative of an impaired humoral immune response. To assay immune function, we used RT-qPCR to quantify AMP expression levels in fat bodies dissected from Canton-S and *P{yolk-GAL4}2/+* females 6 h post-infection with *P. rettgeri*. Concordant with the findings of Kim et al. (2014), we found that infection-induced AMP upregulation was severely attenuated in fat bodies of *P{yolk-GAL4}2* heterozygotes compared to the strong transcriptional induction observed in Canton-S fat bodies (Fig. 4i). Females carrying *P{yolk-GAL4}2* also sustained significantly higher bacterial loads than wild-type animals at 6, 12, and 18 h post-infection (Fig. 4j), suggesting the weakened immune response resulted in failure to contain pathogen growth.

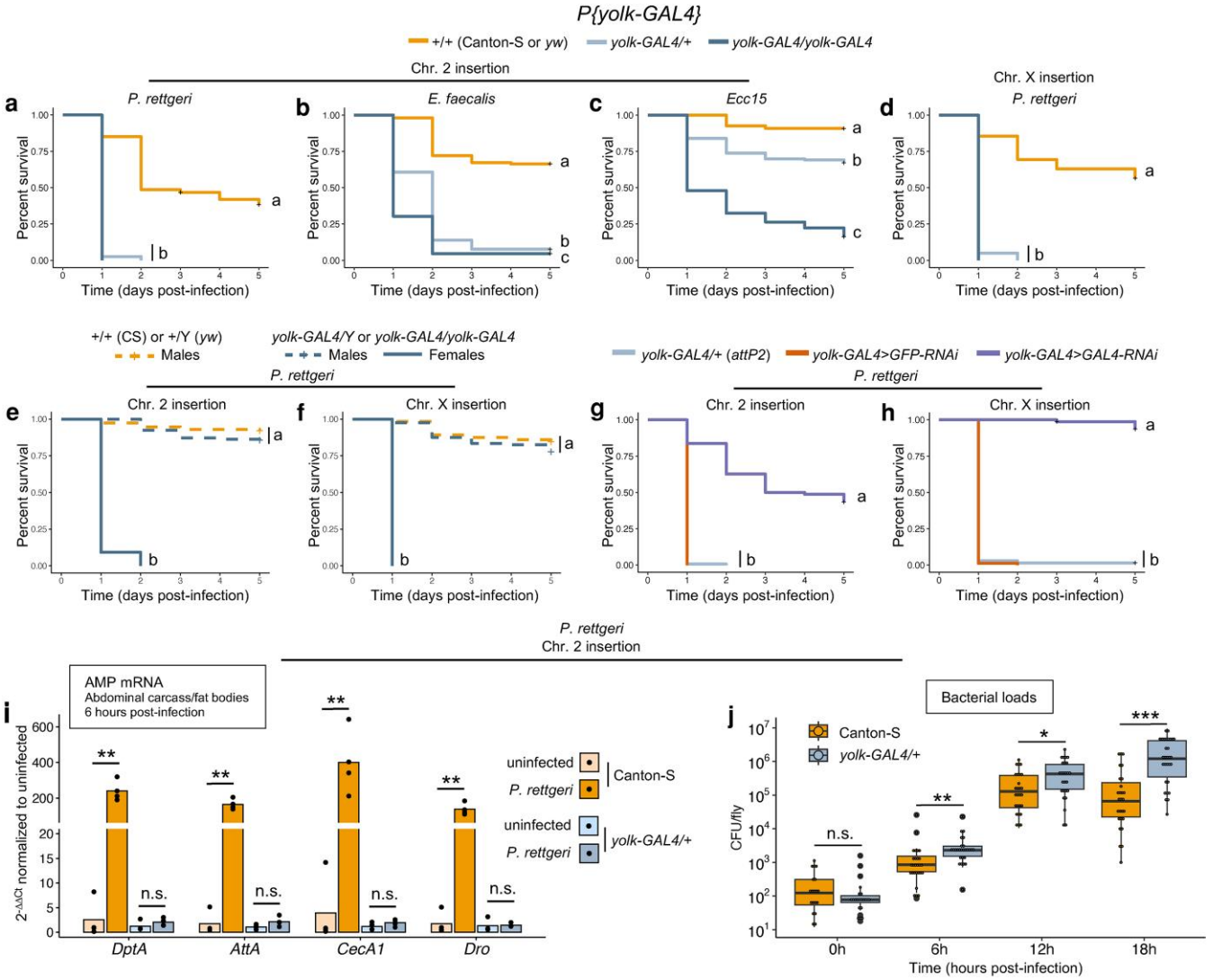

Fig. 4. Expression of *yolk-GAL4* compromises resistance to systemic bacterial infections. (a-c) Females heterozygous or homozygous for the second chromosome *yolk-GAL4* insertion rapidly succumb to systemic infection with *Providencia rettgeri* (A) and *Enterococcus faecalis* (b), and are significantly more susceptible to infection with *Pectobacterium carotovorum* (*Ecc15*; c). d) Heterozygosity or homozygosity for the X chromosome *yolk-GAL4* insertion also causes extreme sensitivity to *P. rettgeri* infection. In panels (a-c) the nontransgenic wild-type control genotype (+/+; orange line) is Canton-S and in panel (d) the control genotype is *yw*. (e,f) Male flies which carry but do not express (see Supplementary Fig. 1h, h') either the second chromosome (e) or X chromosome (f) *yolk-GAL4* insertion survive *P. rettgeri* infection similarly to nontransgenic male flies. (g,h) Knocking down expression of either the second chromosome (g) or X chromosome (h) *yolk-GAL4* insertion by RNAi fully restores females' ability to survive *P. rettgeri* infection. i) Females heterozygous for *yolk-GAL4* fail to upregulate expression of genes coding for antimicrobial peptides following *P. rettgeri* infection. RT-qPCR analysis of abdominal carcasses/fat bodies dissected from unchallenged females or females 6 h post-infection. Data represent $2^{-\Delta\Delta Ct}$ values normalized to the mean ΔC_t value for uninfected samples within each genotype. Each dot represents an individual sample of 10 pooled fat bodies/abdominal carcasses, bars represent the mean. j) Females heterozygous for *yolk-GAL4* sustain higher bacterial loads than nontransgenic control flies over the initial stages of infection with *P. rettgeri*. Each dot represents the bacterial load of an individual fly. Statistics: Infection survival data (a-h) were analyzed by pairwise Log-Rank tests with Benjamini–Hochberg correction for multiple comparisons. Genotypes with different letters are statistically different from one another ($P < 0.05$). RT-qPCR data (i) were analyzed by unpaired two-sample *t*-tests. Bacterial load data (j) were analyzed by Mann–Whitney test (0 h), or by unpaired two-sample tests (6 h, 12, 18 h). $^{*}P < 0.05$, $^{**}P < 0.01$, $^{***}P < 0.001$, n.s. = not significant.

Taken together, these results show the *yolk-GAL4* transgene impairs humoral immune activation in the fat body, resulting in significantly compromised infection resistance.

Fat body *GAL4* expression levels correlate with *P. rettgeri* infection susceptibility

Our results thus far show that *GAL4* expressed under the control of the *yolk* regulatory sequence disrupts energy storage, oogenesis, and infection resistance. We hypothesized that some or all of these traits might be sensitive to *GAL4* expression strength, and that higher levels of *GAL4* in the fat body would result in more severe functional disruption. As a strategy to address this, we presupposed that distinct fat body driver lines might exhibit varied *GAL4* expression levels and that we could use these to test the correlation between transgene expression intensity and fat body-related phenotypes. We therefore examined 4 additional *GAL4* lines commonly used for genetic manipulations in the fat body: *3.1Lsp2-GAL4*, *C564-GAL4*, r^4*-GAL4*, and *Lpp-GAL4* (Table 1).

To confirm that the drivers we selected are all expressed in the adult fat body and to assess their tissue specificity, we first crossed each line to a *UAS-mCD8::GFP* reporter and visualized their

Table 1. Fat body *GAL4* driver lines.

Transgene	Regulatory sequence description	Source reference
3.1Lsp2-GAL4	3.1kbp promoter fragment upstream of *Lsp2* gene coding sequence	Lazareva et al. (2007)
C564-GAL4	Second chromosome *P{GawB}* enhancer trap	Manseau et al. (1997)
r^4*-GAL4*	Tetrameric repeat of the "r" element from the *yolk* regulatory sequence	Lee and Park (2004)
Lpp-GAL4	*GAL4* coding sequence flanked by 5.5kbp promoter fragment and 3kbp 3′UTR fragment of the *apolpp* gene	Brankatschk and Eaton (2010)

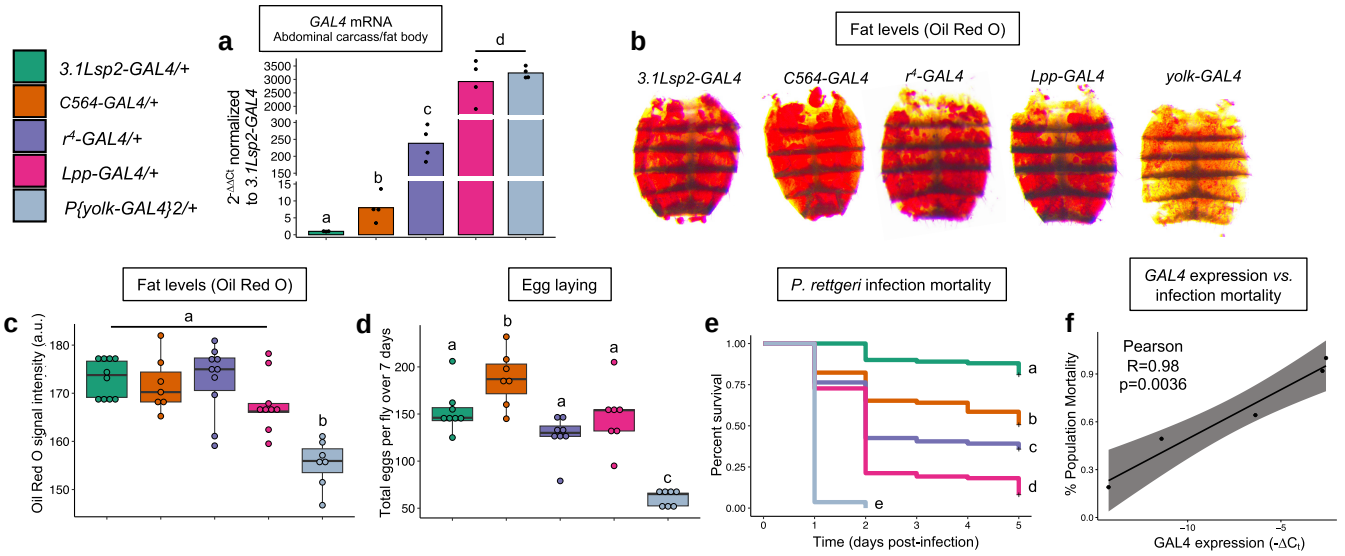

Fig. 5. *GAL4* expression in the adult fat body correlates with *P. rettgeri* infection sensitivity. a) RT-qPCR analysis documents a range of *GAL4* expression levels in abdominal carcasses dissected from females heterozygous for different fat body driver transgenes. Data represent $2^{-\Delta\Delta Ct}$ values normalized to the mean ΔC_t value for *3.1Lsp2-GAL4/+* flies. Each dot represents an individual sample of 10 pooled fat bodies/abdominal carcasses, bars represent the mean. b) Representative images of Oil Red O-stained abdominal carcasses dissected from females heterozygous for each of the indicated *GAL4* transgenes. c) Quantification of Oil Red O staining intensities indicates that only *yolk-GAL4* results in decreased abdominal lipid levels while the other drivers do not differ in fat content. Each dot represents an individual fly/abdomen, a.u.=arbitrary units. d) Additional fat body driver transgenes do not result in reduced egg laying rates comparable to *yolk-GAL4*. Each dot represents an individual replicate, 2 to 3 females per replicate. (e,f) Across the 5 *GAL4* transgenes assayed, mortality induced by *P. rettgeri* infection (e) directly correlates with *GAL4* expression levels in the fat body (f). The correlation analysis in (f) plots the percentage of flies that succumbed by 5 d post-infection (*y*-axis; from data represented in (e)) against *GAL4* expression levels (x-axis; from data represented in (a)), quantified as the negative average ΔC_t value (C_{tGAL4}–C_{tRpl32}; increasing value indicates higher *GAL4* expression). Statistics: Oil Red O signal intensity data (c) and egg laying data (d) were analyzed by one-way ANOVA with Tukey's post hoc pairwise comparisons. Infection survival data (e) were analyzed by pairwise Log-Rank test with Benjamini–Hochberg correction for multiple comparisons. Genotypes with different letters are statistically different from one another ($P < 0.05$).

expression patterns across major adult tissues in young adult females (Supplementary Fig. 4). As expected, all 4 lines induced GFP expression in the abdominal fat body (Supplementary Fig. 4ba, ca, da, ea). Notably, *3.1Lsp2-GAL4* produced an extremely faint, almost undetectable live fluorescent signal at 25 °C (Supplementary Fig. 4aa), but drove a mosaic pattern of fat body GFP expression when flies were housed at 29 °C (Supplementary Fig. 4ba), which increases GAL4 activity (Duffy 2002). Consistent with prior reports (Lazareva et al. 2007; Brankatschk and Eaton 2010; Armstrong et al. 2014), *3.1Lsp2-GAL4* and *Lpp-GAL4* induced highly specific fat body expression (Supplementary Fig. 4ba, ea), with no visible GFP fluorescence in the brain, flight muscle, gut, Malpighian tubules, or ovaries (Supplementary Fig. 4ab–af, bb–bf, eb–ef). In addition to the fat body (Supplementary Fig. 4ca, da), *C564-GAL4* and *r*^{4}*-GAL4* both produced regionalized GFP expression in the gut (Supplementary Fig. 4cd, ce, dd, de), though not in other tissues (Supplementary Fig. 4cb, cc, cf, db, dc, df). *C564-GAL4* activated GFP expression in the anterior midgut (Supplementary Fig. 4cd), and a middle midgut region which, based on its position and morphology, we suspect spans the stomach-like R3 compartment (Supplementary Fig. 4ce; Buchon et al. 2013). The *r*^{4}*-GAL4* driver activated GFP expression in the proventriculus and crop duct (Supplementary Fig. 4dd), and throughout the hindgut (Supplementary Fig. 4de).

After confirming each driver's expression pattern, we next directly measured transgene expression strength by quantifying *GAL4* transcript levels in the fat body. To accomplish this, we crossed *3.1Lsp2-GAL4*, *C564-GAL4*, *r*^{4}*-GAL4*, *Lpp*-GAL4, or *yolk-GAL4* to Canton-S flies, and used RT-qPCR to quantify *GAL4* expression in fat bodies dissected from the resulting female progeny heterozygous for each transgene. As we anticipated, this analysis revealed considerable variation in fat body *GAL4* transcript levels across the 5 lines. Consistent with our imaging results (Supplementary Fig. 4aa, ba), we found that *3.1Lsp2-GAL4* flies expressed *GAL4* at the lowest levels relative to the other 4 lines (Fig. 5a). Relative to *3.1Lsp2-GAL4* as a baseline, *GAL4* expression was, on average, 8-fold higher in fat bodies of *C564-GAL4* flies and 238-fold higher in *r*^{4}*-GAL4* flies (Fig. 5a). *Lpp-GAL4* and *yolk-GAL4* displayed the strongest fat body *GAL4* expression, with both exhibiting >2,900-fold higher mRNA relative to *3.1Lsp2-GAL4* (Fig. 5a).

Having documented a wide range of *GAL4* transcript levels across our 5 selected drivers and noting that *yolk-GAL4* was one

of the highest-expressing lines, we leveraged this variation to ask whether *GAL4* expression strength determines the severity of impacts on fat body-regulated traits. We measured fat levels, egg laying, and mortality from *P. rettgeri* infection in females carrying each of the 5 *GAL4* transgenes, again examining heterozygous progeny from crosses to Canton-S.

We found no significant correlation between *GAL4* expression levels and fat levels or egg output across driver lines. ORO lipid staining intensities were not significantly different among flies heterozygous for *3.1Lsp2-GAL4/+*, *C564-GAL4/+*, r^4*-GAL4/+*, and *Lpp-GAL4/+*, although all were higher than *yolk-GAL4/+* females (Fig. 5, b and c). Similarly, egg output was comparable among females carrying *3.1Lsp2-GAL4*, r^4*-GAL4*, and *Lpp-GAL4*, with *C564-GAL4/+* females laying more eggs than any other line, and *yolk-GAL4/+* females again producing relatively low numbers of eggs (Fig. 5d). However, we observed a striking correlation between *GAL4* expression levels and susceptibility to *P. rettgeri* infection (Fig. 5, e and f). Flies heterozygous for *3.1Lsp2-GAL4*, which express the lowest *GAL4* levels (Fig. 5a), were the least susceptible to infection, with only ~15% of the total population succumbing. *C564-GAL4/+* and r^4*-GAL4/+* flies displayed intermediate susceptibility, with ~40% and ~50% death, respectively (Fig. 5e). *Lpp-GAL4*, which is expressed comparably to *yolk-GAL4* (Fig. 5a), caused relatively high mortality (~80%), though not as severe as the 100% lethality of *yolk-GAL4/+* females (Figs. 4, a and and 5e).

To further confirm that *GAL4* levels impact infection survival, we knocked down *GAL4* expression in female *Lpp-GAL4* heterozygotes (Supplementary Fig. 5a). As with *yolk-GAL4*, reducing *Lpp-GAL4* expression by RNAi significantly increased *P. rettgeri* infection survival (Supplementary Fig. 5b). Because *Lpp-GAL4* is expressed in flies of both sexes, we also examined *GAL4* levels and infection mortality in *Lpp-GAL4* heterozygous males. We found that *Lpp-GAL4/+* males expressed significantly less *GAL4* than genetically matched females (Supplementary Fig. 5c) and exhibited minimal infection-induced mortality (Supplementary Fig. 5d). We note, however, that sexual dimorphism in survival of *P. rettgeri* infection has previously been reported (Duneau et al. 2017) with males being more resistant to infection even in the absence of transgene expression.

In summary, our data show that sensitivity to *P. rettgeri* infection quantitatively scales with *GAL4* expression in the adult female fat body, but stored fat levels and egg production do not. Nevertheless, expression of *GAL4* in the fat body controlled by the *yolk* enhancer impacts all three traits, so in our subsequent experiments, we sought to investigate potential mechanisms by which this might occur.

No evidence for GAL4-induced apoptosis in the adult female fat body

High levels of GAL4 have been reported to induce apoptosis in eye imaginal discs (Kramer and Staveley 2003) and in ventral lateral neurons of the adult brain (Rezával et al. 2007). We therefore hypothesized that overexpression of GAL4 might induce cell death in the fat body, which could contribute to the physiological dysfunction we documented in *yolk-GAL4* expressing flies. If the reduced infection resistance, egg production, and fat storage phenotypes caused by *yolk-GAL4* were due to fat body cell death, we reasoned that genetically inhibiting apoptosis should suppress these phenotypes. To test this, we crossed *yolk-GAL4* with flies carrying a *UAS* transgene encoding Baculovirus p35 protein, which potently inhibits apoptosis-activating caspases Dcp1 and Death-related ICE-like caspase (Drice; Supplementary Fig. 6a; Hay et al. 1994; Hawkins et al. 2000; Meier et al. 2000; Lannan et al. 2007). Compared to control animals expressing a nonfunctional *UAS-eGFP* transgene, we found that p35 expression did not increase fat levels (Supplementary Fig. 6b, b′, c), egg output (Supplementary Fig. 6d), or infection resistance (Supplementary Fig. 6e) in *yolk-GAL4* heterozygotes. In fact, *yolk-GAL4 > p35* females displayed a modest decrease in egg production relative to *yolk-GAL4 > eGFP* controls (Supplementary Fig. 6d). Successful completion of oogenesis requires apoptotic elimination of the follicle cells in late-stage oocytes (Nezis et al. 2002). Inhibition of this process by p35 might exacerbate the oogenesis defects in *yolk-GAL4* females. These results do not support the hypothesis that GAL4-induced apoptosis contributes to the deleterious phenotypes of *yolk-GAL4*-expressing flies.

Expressing nuclear-localized mCherry in the fat body reduces infection survival

We next asked whether high-level expression of transgenic proteins in general can affect fat body function, or whether the metabolic, reproductive, and immune phenotypes of *yolk-GAL4*-expressing flies are specifically caused by the GAL4 protein. We formulated 2 distinct hypotheses to explain how strong transgene expression might generally impact the fat body's ability to execute key cellular and physiological functions. H1: Because the GAL4 transcription factor is actively imported into the nucleus (Uv et al. 2000), we hypothesized that import and/or accumulation of high levels of foreign protein in the nucleus might disrupt essential cellular processes like chromatin organization or gene expression, which would be consistent with the reduced expression of *Yolk Protein* (Fig. 3g) and AMP genes (Fig. 4i) we observed in *yolk-GAL4/+* fat bodies. H2: As a nonexclusive alternative, we hypothesized that expressing high levels of transgenic protein might exhaust cellular resources and overwhelm endogenous cellular machinery, thus impairing the fat body's capacity to perform critical functions. We reasoned that if either of these proposed mechanisms were responsible for the defects we observed in *yolk-GAL4*-expressing flies, then high-level transgenic expression of other nuclear-localized proteins might elicit similar phenotypes. However, the 2 hypotheses can be distinguished. If general cellular strain caused by high-level expression of transgenic products (H2) impairs the fat body's metabolic, reproductive, or immune functions, then expressing either a cytoplasmic or a nuclear-localized transgenic protein in the fat body would result in phenotypes similar to those of *yolk-GAL4*. Alternatively, if nuclear import and/or accumulation of the transgenic protein (H1) primarily affects these physiological traits, we would expect other nuclear-localized transgenic proteins to phenocopy *yolk-GAL4* but the same transgenic protein would have no effect if it remained localized to the cytoplasm.

To resolve these alternatives, we generated 2 new transgenic fly lines in which the *yolk* enhancer sequence directs expression of the fluorescent protein mCherry. The 2 lines are identical except one construct includes N- and C-terminal nuclear localization signal sequences (*yolk-mCherry.nls*), while the other lacks these sequences (*yolk-mCherry.cyt*). Both *yolk-mCherry.nls* and *yolk-mCherry.cyt* were integrated at the same *attP40* docking site on the second chromosome, enabling us to directly compare the effects of nuclear import versus protein synthesis on metabolic, reproductive, and immune physiology. We selected mCherry as an alternative transgenic protein to test our hypotheses for 2 reasons. First, mCherry allowed us to easily assess expression and subcellular localization by fluorescence microscopy. Second, in the event that fly physiology was not strongly affected, we reasoned that these lines would constitute novel transcriptional reporters broadly useful for *Drosophila*

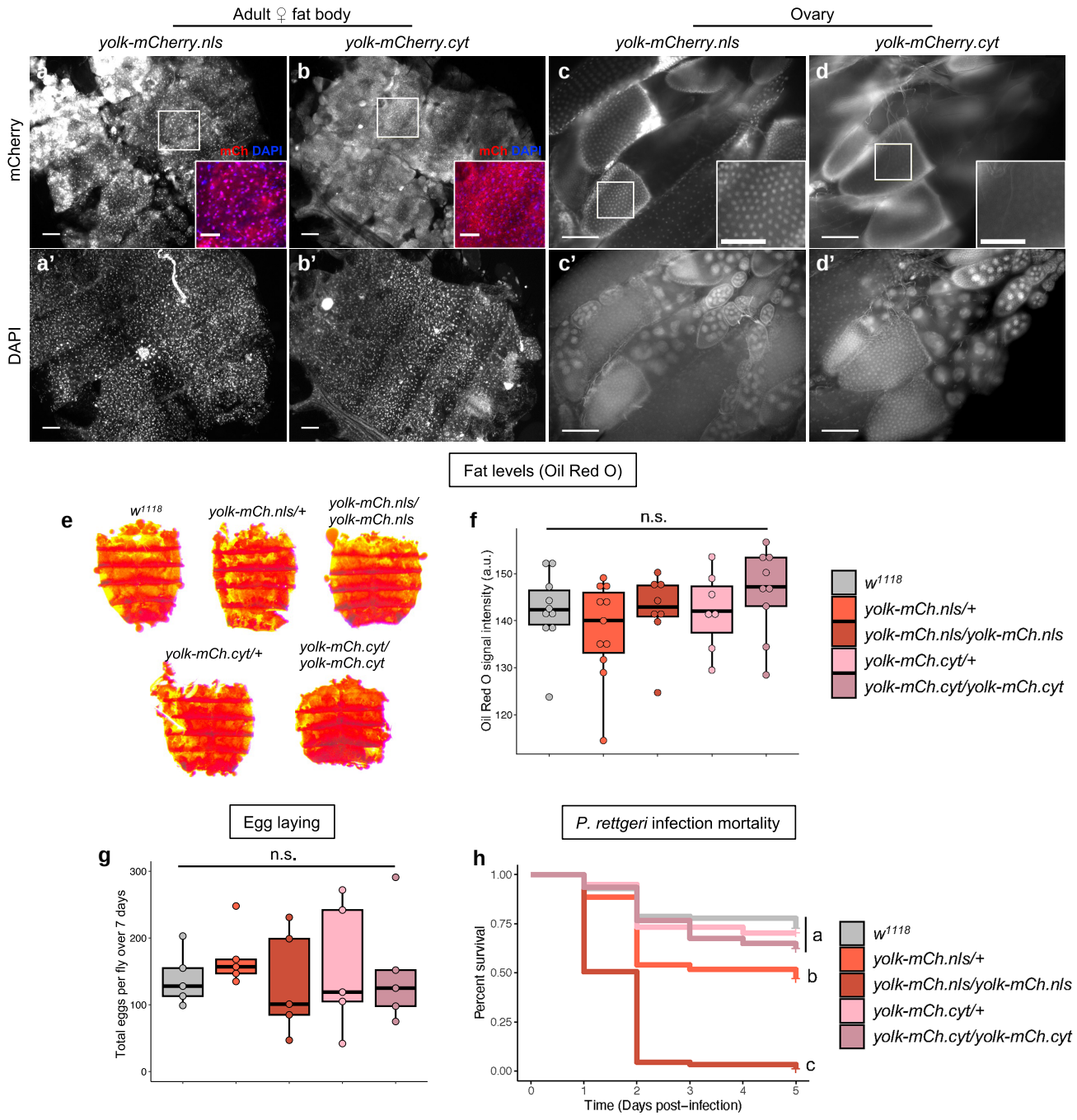

Fig. 6. Nuclear-localized mCherry expressed in the fat body with the *yolk* enhancer reduces infection survival but not lipid levels or egg laying. (a-d') The *yolk-mCherry* transgenes are expressed in the adult female fat body (a-b') and in ovarian follicle cells (c-d'). The *yolk-mCherry.nls* construct, with nuclear-localization sequences flanking mCherry, shows strongly nuclear-localized mCherry signal in the fat body (a), while the *yolk-mCherry.cyt* transgene produces mCherry signal more diffuse in the cytoplasm (b). Insets show merged mCherry and DAPI signal to visualize nuclear (a) vs cytoplasmic (b) localization. In mid-stage follicle cells localized mCherry signal is stronger for *yolk-mCherry.nls* (c) than for *yolk-mCherry.cyt* (d). All mCherry images were acquired with identical imaging settings. Insets show mCherry signal alone. Nuclei are stained with DAPI (a', b', c', d') to reveal overall tissue morphology. Scale bars = 100 µm, inset scale bars = 50 µm. (e,f) Expressing cytoplasmic or nuclear-localized mCherry under control of the yolk enhancer does not affect abdominal lipid levels. e) Representative images of Oil Red O-stained abdominal carcasses dissected from w^{1118} control females or from females heterozygous or homozygous for either *yolk-mCherry.nls* or *yolk-mCherry.cyt*. f) Quantification of ORO staining intensity. Each dot represents an individual fly/abdomen, a.u. = arbitrary units. g) Females heterozygous or homozygous for either *yolk-mCherry* construct lay comparable numbers of eggs to nontransgenic control females. Each dot represents an individual replicate, 2 to 3 females per replicate. h) Females expressing nuclear-localized mCherry in the fat body exhibit transgene dose-dependent increased mortality caused by *P. rettgeri*, with one copy of *yolk-mCherry.nls* moderately increasing infection sensitivity relative to w^{1118} controls and *yolk-mCherry.nls* homozygotes exhibiting high susceptibility to infection. Cytoplasmically retained mCherry produced in the same expression pattern does not affect females' susceptibility to *P. rettgeri* infection, with *yolk-mCherry.cyt* heterozygotes and homozygotes surviving comparably to w^{1118} females. Statistics: ORO data (f) and egg laying data (g) were analyzed by one-way ANOVA. Infection survival data (h) were analyzed by pairwise Log-Rank test with Benjamini–Hochberg correction for multiple comparisons. Genotypes with different letters are statistically different from one another ($P < 0.05$), n.s. = not significant.

researchers studying mechanisms of enhancer activation and *yolk* gene regulation.

To confirm their expression patterns, we first visually examined mCherry fluorescence in tissues dissected from *yolk-mCherry.nls* and *yolk-mCherry.cyt* flies (Fig. 6a–d′, Supplementary Fig. 7). As expected, both lines exhibited robust mCherry signal throughout the adult female fat body (Fig. 6a–b′, Supplementary Fig. 7a, a′, g, g′), and in the ovarian follicle cells (Fig. 6c–d′, Supplementary Fig. 7b, b′, h, h′). Additionally, mCherry was strikingly nuclear-localized in fat bodies of *yolk-mCherry.nls* females (Fig. 6a), in contrast to the more diffuse fluorescence observed in *yolk-mCherry.cyt* fat bodies (Fig. 6b). In follicle cells of *yolk-mCherry.nls* females, mCherry signal also showed strong nuclear localization (Fig. 6c). We observed some localized fluorescence in *yolk-mCherry.cyt* follicle cells (Fig. 6d), but the signal was less pronounced than in *yolk-mCherry.nls* follicles. Notably, unlike *yolk-GAL4* (Supplementary Fig. 1e, j), we did not observe mCherry signal in the crop duct for either line (Supplementary Fig. 7e, e′, k, k′). We also did not detect fluorescence in the brain, gut, Malpighian tubules, or muscle (Supplementary Fig. 7c–f′, i–l′), nor in the fat bodies of late third instar female larvae (Supplementary Fig. 7m, m′, o, o′) or adult males (Supplementary Fig. 7n, n′, p, p′). Thus, our *mCherry* transgenes largely recapitulate the spatiotemporal expression patterns of *yolk-GAL4* and display the expected subcellular localization of fluorescent protein.

Having validated their expression, we used these new fly lines to ask whether overexpression and/or nuclear import of an alternative transgenic protein distinct from GAL4 might also impact metabolism, reproduction, or immunity. To accomplish this, we measured abdominal fat levels, egg laying rates, and survival of *P. rettgeri* infection in females heterozygous or homozygous for *yolk-mCherry.cyt* or *yolk-mCherry.nls*. Because *yolk-GAL4* produced strong phenotypes when heterozygous over a variety of genetic backgrounds, we examined *yolk-mCherry* heterozygotes both in *trans* to their w^{1118} background and to the Canton-S genotype used for our prior analyses.

We found that fat body lipid levels and reproductive output were not affected by either mCherry transgene. Abdominal lipid staining with ORO appeared robust in females heterozygous or homozygous for *yolk-mCherry.nls* or *yolk-mCherry.cyt* and quantified staining intensities were statistically equivalent to those of nontransgenic control flies (Fig. 6, e and f, Supplementary Fig. 8a, b). Similarly, females carrying *yolk-mCherry.nls* or *yolk-mCherry.cyt* did not display any reduction in egg laying compared to control females (Fig. 6g, Supplementary Fig. 8c). However, when challenged with *P. rettgeri*, we found that *yolk-mCherry.nls* reduced female's capacity to survive infection in a transgene dose-dependent manner (Fig. 6h, Supplementary Fig. 8d). Females heterozygous for *yolk-mCherry.nls* over both w^{1118} and Canton-S backgrounds displayed moderately but significantly increased infection-induced mortality (Fig. 6h, Supplementary Fig. 8d). By comparison, *yolk-mCherry.nls* homozygous females were highly susceptible to *P. rettgeri*, with >95% of the population succumbing by 24 to 48 h post-infection (Fig. 6h). In contrast, the *yolk-mCherry.cyt* transgene, producing the same mCherry protein localized to the cytoplasm, had no effect on infection mortality when heterozygous or homozygous compared to the w^{1118} background control line (Fig. 6h). When heterozygous over the Canton-S background, *yolk-mCherry.cyt* led to a small but significant reduction in infection survival, equivalent to that caused by *yolk-mCherry.nls* in *trans* to Canton-S (Supplementary Fig. 8d). This suggests that *mCherry* expression alone might exert modest deleterious effects on infection susceptibility in certain genetic backgrounds, but nuclear localization of copious transgenic protein results in substantial sensitivity to infection.

In summary, these results show that expression of mCherry under control of the *yolk* enhancer does not by itself strongly impact fat-body-regulated physiological traits, but that nuclear import of mCherry dramatically increases susceptibility to infection without affecting fat stores or egg output. Our results therefore suggest that metabolism and oogenesis might be disrupted by *GAL4* expression specifically, while the ability to withstand infection might be more generally sensitive to nuclear-localized transgenic proteins expressed in the fat body.

Conversion of *yolk-GAL4* into *yolk-LexA* alleviates physiological defects caused by *GAL4* expression

Given our observation that nuclear-localized GAL4 and mCherry reduced infection survival in a transgene dose-dependent manner (Figs. 4, b and c, 5, e and and 6h), we predicted that another nuclear-localized transgenic protein might similarly reduce infection survival without impacting fat levels or egg laying. To test this prediction, we applied Homology-Assisted CRISPR Knock-in (HACK; Lin and Potter 2016; Chang et al. 2022; Rankin et al. 2024) to *yolk-GAL4* flies in order to replace the *GAL4* coding sequence with a *LexA* transgene (Fig. 7a, Supplementary Fig. 9a). We reasoned that generating a new fly line in which the exact *yolk* regulatory sequence of the original stock directs LexA expression would provide another tool to ask whether infection resistance can be broadly perturbed by nuclear-localized transgenic proteins. In addition, *yolk-LexA* would constitute a novel reagent useful for adult female fat body-specific genetic manipulations.

Using a recently developed, efficient HACK donor (Rankin et al. 2024), we converted *yolk-GAL4* on the second chromosome into a *yolk-LexA* transgene. As expected, *yolk-LexA* drove robust GFP expression in the same pattern as *yolk-GAL4* when crossed to a *LexAop-mCD8::GFP* responder line (Fig. 7b) but failed to activate *UAS-mCD8::GFP* (Fig. 7b′), indicative of successful transgene conversion. This new line allowed us to ask whether an alternative, nuclear-localized transcription factor expressed from the identical genomic locus of the *P{yolk-GAL4}2* insertion would also affect fat levels, egg laying, or infection survival. We examined these traits in females heterozygous or homozygous for *yolk-LexA* in the *yw* genetic background in which they were constructed, and also in F1 heterozygotes from crosses with Canton-S.

We found that females heterozygous or homozygous for *yolk-LexA* did not exhibit reduced fat stores relative to nontransgenic controls (Fig. 7, d and e). In fact, abdominal ORO staining levels were higher in females carrying 1 or 2 copies of *yolk-LexA* (Fig. 7, d′ and d″) compared to their *yw* background line (Fig. 7, d and e). We also found that *yolk-LexA* had no effect on egg output, with heterozygotes and homozygotes laying total egg numbers comparable to those of *yw* females over 7 d post-eclosion (Fig. 7f). Similarly, females carrying *yolk-LexA* heterozygous over the Canton-S background displayed no reduction in abdominal fat levels (Supplementary Fig. 9b, c) or egg production (Supplementary Fig. 9d).

In contrast to fat levels and egg laying, we observed a dose-dependent effect of *yolk-LexA* on females' sensitivity to *P. rettgeri* infection, similar to that observed with *yolk-mCherry.nls*. One copy of *yolk-LexA* heterozygous over the *yw* genetic background had no effect on infection mortality (Fig. 7g). When heterozygous over the Canton-S background, *yolk-LexA* led to significantly reduced infection survival compared to nontransgenic controls (Supplementary Fig. 9e). However, ~50% of these *yolk-LexA* heterozygotes were

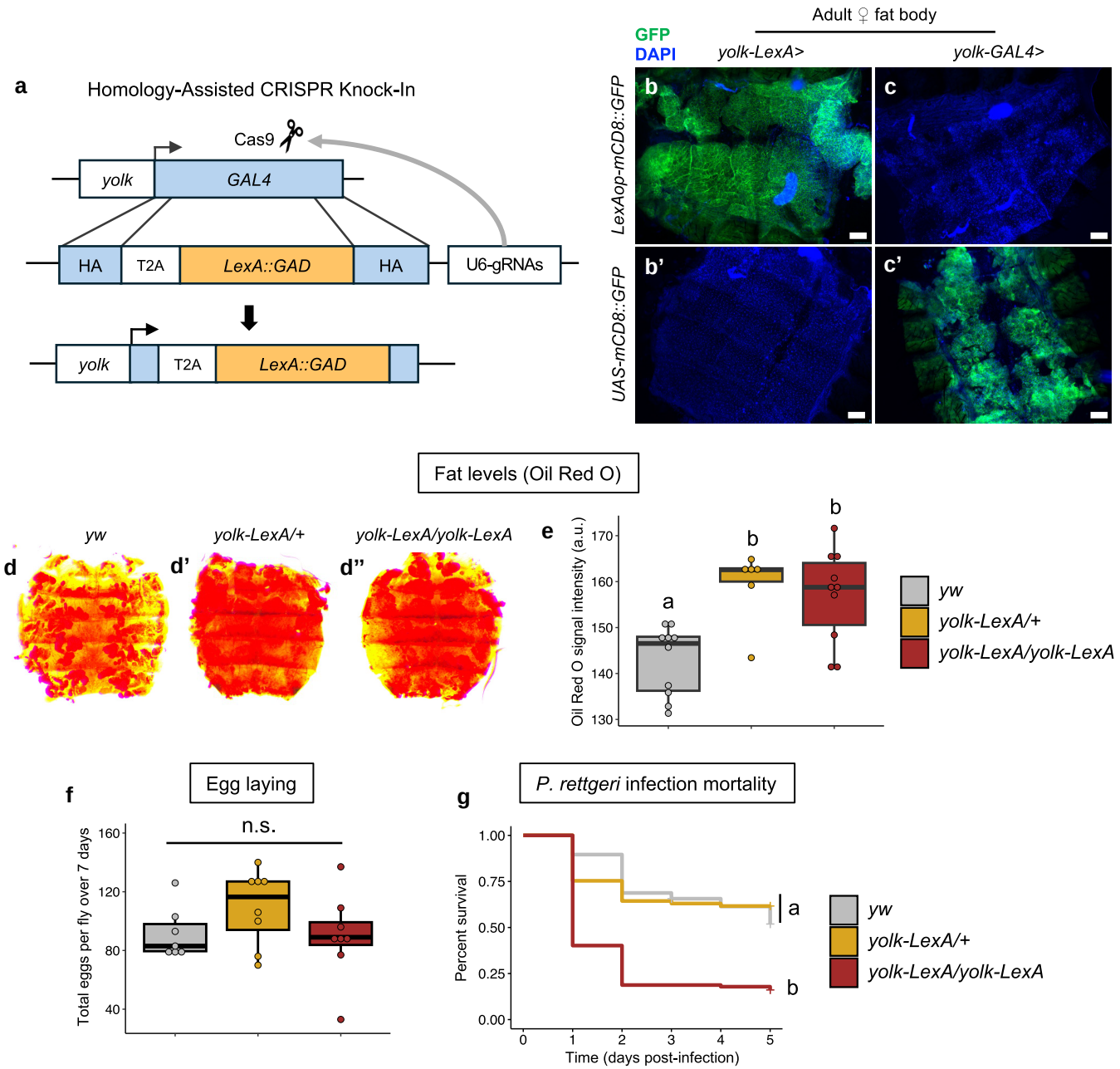

Fig. 7. Converting *yolk-GAL4* to *yolk-LexA* alleviates metabolic and reproductive phenotypes, and lessens infection sensitivity caused by *GAL4* expression. a) Schematic illustrating the HACK approach (Lin and Potter 2016; Rankin et al. 2024) for in vivo CRISPR-mediated conversion of the second chromosome *yolk-GAL4* line into *yolk-LexA*. (b-c') The converted *yolk-LexA* line activates expression of a *LexAop-mCD8::GFP* reporter in the adult female fat body (b) but does not activate expression of a *UAS-mCD8::GFP* reporter (b'), indicating successful transgene conversion. The original *yolk-GAL4* transgene does not activate the *LexAop-mCD8::GFP* transgene (c) but does induce *UAS-mCD8::GFP* expression (c'). Nuclei are labeled with DAPI to reveal general tissue morphology. Scale bars = 100 µm. (d-e) Unlike *yolk-GAL4* (Fig. 2, Supplementary Fig. 2), females carrying *yolk-LexA* do not display reduced abdominal lipid levels revealed by ORO staining. ORO signal is stronger in abdomens from flies with *yolk-LexA* than in *yw* background controls. In panel (e), each dot represents an individual fly/abdomen, a.u. = arbitrary units. f) Females heterozygous or homozygous for *yolk-LexA* lay numbers of eggs comparable to those of nontransgenic *yw* females. Each dot represents an individual replicate, 2 to 3 females per replicate. g) Heterozygosity for *yolk-LexA* does not affect survival of *P. rettgeri* infection, while *yolk-LexA* homozygotes are more susceptible to infection. ORO data (d) were analyzed by Kruskal–Wallis test with Dunn's post hoc pairwise comparisons. Egg laying data (e) were analyzed by one-way ANOVA. Infection survival data (f) were analyzed by pairwise Log-Rank tests with Benjamini–Hochberg correction for multiple comparisons. Genotypes with different letters are statistically different from one another ($P < 0.05$), n.s. = not significant.

able to survive *P. rettgeri* infection, in striking contrast to the complete population mortality of *yolk-GAL4* heterozygotes (Supplementary Fig. 9e). Notably, *yolk-LexA* homozygous females experienced substantially greater infection-induced mortality compared to heterozygous and control females (Fig. 7g). Again, though, the infection sensitivity caused by 2 copies of *yolk-LexA* was less than that caused by a single copy of *yolk-GAL4*, as ~15% to 20% of *yolk-LexA* homozygotes consistently survived infection (Fig. 7g).

These data add further evidence that nuclear-localized transgenic proteins expressed at high levels in the adult fat body generally compromise the ability of *Drosophila* to survive pathogenic infection. Additionally, these results reinforce the conclusion

that fat storage and egg production are more specifically affected by *GAL4* expression, as exchanging *GAL4* for *LexA* fully alleviates the metabolic and reproductive phenotypes caused by *yolk-GAL4*.

Discussion

Our study raises important considerations about the effects of transgenic tools on tissue homeostasis in *Drosophila* and other genetically manipulated organisms, and about the limits on cellular function imposed by high levels of non-native proteins.

Several nonexclusive mechanisms might explain how high levels of transgenic GAL4 in fat body cells result in disrupted tissue integrity, and reduced lipid levels, egg production, and infection resistance. The fat body simultaneously executes biologically varied and energetically demanding processes, including synthesis and breakdown of macromolecular stores and secretion of large quantities of proteins, endocrine molecules, and metabolites (Canavoso et al. 2001; Arrese and Soulages 2010; Zheng et al. 2016). Allocation of a finite set of molecular resources among these processes can, in some cases, overburden the functional capacity of the fat. For example, mating-induced protein synthesis has been shown to constrain the fat body's ability to mount an immune response, leading to activation of stress responses characteristic of overburdened translational capacity (Gupta et al. 2022). The demands of synthesizing large quantitates of GAL4 or other transgenic proteins at high levels might divert adipocyte resources from producing molecules required for metabolism, reproduction, and immunity. Additionally, high-level production of superfluous protein could overwhelm the functional capacities of core cellular machinery and organelles, leading to activation of stress responses that arrest overall tissue function.

We only observed poor tissue integrity, reduced fat stores, and low egg output in females expressing *yolk-GAL4*, while flies expressing *GAL4* from other fat body promoters did not exhibit these defects. Notably, this includes the *Lpp-GAL4* transgene, which expressed *GAL4* comparably to *yolk-GAL4* but had a weaker impact on infection survival and did not affect the other measured traits. While *GAL4* expression is comparable between these drivers 7 d post-eclosion, *yolk-GAL4* might express more strongly at earlier adult stages. The adult fat body completes maturation over the first few days following eclosion (Johnson and Butterworth 1985; Aguila et al. 2007; Lei et al. 2023; Tsuyama et al. 2023). Higher GAL4 levels during this period might disrupt final fat body development, causing the poor tissue integrity we observed exclusively in *yolk-GAL4* flies. Our data also suggest that *GAL4* expression in follicle cells might contribute to oogenesis and egg laying defects in *yolk-GAL4* flies, whereas *Lpp-GAL4* and the other drivers we examined were not visibly expressed in the ovary.

Our observation that mCherry, and LexA had a less severe impact on fat body-regulated traits suggests that GAL4 protein might exert unique cytotoxic effects. Because the LexA::GAD fusion protein includes the GAL4 activation domain, our results suggest that whatever specific attributes of GAL4 induce toxicity likely involve the C-terminal DNA binding domain, or properties only conferred by the full protein conformation. Previous studies have suggested that GAL4 can disrupt cellular protein homeostasis and quality control mechanisms. In a microarray analysis, Liu and Lehmann (2008) identified protein ubiquitination factors as overrepresented among the GAL4-responsive genes in larval salivary glands. The muscle-specific MHC-GeneSwitchGAL4 transgene was recently shown to cause age-dependent accumulation of polyubiquitinated protein aggregates in adult flight muscles, although these effects required activation by RU486 feeding (Zappia et al. 2024). Similarly, Rezával et al. (2007) found high levels of GAL4 in insoluble protein extracts from heads of aged flies expressing *pdf-GAL4*. Future studies should consider whether GAL4 might disrupt cellular functions in the fat body by similar mechanisms.

We found that 3 distinct nuclear-localized transgenic proteins —GAL4, mCherry, and LexA—reduced flies' capacity to survive systemic bacterial infection. We observed that the identical mCherry protein expressed from the same genomic locus and in the same tissue-specific pattern but lacking nuclear localization sequence had no effect on infection mortality. As we did not quantify protein level, we cannot rule out the possibility that *yolk-mCherry.cyt* flies might sustain lower levels of mCherry protein than *yolk-mCherry.nls* flies. Nevertheless, our data suggest the presence of transgenic proteins in fat body nuclei can strongly impact infection sensitivity. In *Drosophila* and other insects, systemic microbial infections activate a broadly conserved humoral immune response that is predominantly regulated by the Immune Deficiency (IMD) and Toll signaling pathways. These pathways comprise intracellular signaling cascades that culminate in the nuclear translocation of the NF-κB family transcription factors Relish (Rel), Dorsal-related immunity factor (Dif), and Dorsal (Dl). On entering the nucleus, these transcription factors massively upregulate the expression of AMPs that are then secreted from the fat body into the hemolymph to kill the pathogen (De Gregorio et al. 2002; Valanne et al. 2011; Myllymäki et al. 2014; Troha et al. 2018; Westlake et al. 2025). In the larval fat body, a specific nucleoporin encoded by the gene *members only* (*mbo*, homologous to vertebrate *Nup88*) is required for nuclear import of Rel, Dif, and Dl upon infection (Uv et al. 2000). Interestingly, *mbo* is also required for nuclear localization of GAL4 (Uv et al. 2000). Our data are consistent with a model where high levels of nuclear-localized transgenic proteins might oversaturate nuclear pore channels, such as those formed with mbo, and physically impede the infection-induced nuclear translocation of NF-κBs resulting in abrogated or delayed AMP production and consequent failure to constrain pathogen proliferation. In further support of this model, we and Kim et al. (2014) found that infected flies expressing *yolk-GAL4* display markedly reduced AMP gene upregulation, which could reflect impaired nuclear import of Rel. The potential for GAL4 and other nuclear-localized transgenic proteins to affect nuclear import and function of native transcription factors warrants further investigation.

In conducting this study, we generated several new *D. melanogaster* lines that will be broadly useful to the *Drosophila* research community. Our *yolk-mCherry* lines faithfully recapitulate the well-documented spatiotemporal and sex-specific expression patterns of the *yolk* enhancer, and effectively re-create historical *yolk-lacZ* reporter lines that yielded fundamental discoveries about mechanisms of enhancer regulation (Coschigano and Wensink 1993; An and Wensink 1995a,b) but, to the best of our knowledge, are now lost. Both *yolk-mCherry.nls* and *yolk-mCherry.cyt* provide robust, easily-visualized fluorescent readouts of *yolk* enhancer activity, and could be used as indicators for studying processes such as sex determination (Belote et al. 1985; Bownes 1994; Tarone et al. 2012), nutrient sensing systems (Bownes and Blair 1986; Bownes et al. 1988; Terashima et al. 2005), and endocrine signaling (Jowett and Postlethwait 1980; Bownes et al. 1987, 1996). In addition to these reporters, we used HACK (Lin and Potter 2016; Chang et al. 2022; Rankin et al. 2024) to convert *yolk-GAL4* into *yolk-LexA*, which can be used in genetic experiments employing the *LexA/LexAop* binary expression system (Lai and Lee 2006). Crucially, and in striking contrast to *yolk-GAL4*, heterozygosity for *yolk-LexA* (as would be the case in

most experimental setups) did not reduce fat levels or egg production, and had little or no effect on infection sensitivity. We have therefore generated a reagent that retains the major advantages of inherent adult female-specific expression conferred by the *yolk* enhancer, but which lacks the extreme deleterious effects on fly physiology caused by *yolk-GAL4*. As such, the *yolk-LexA* line constitutes a valuable new tool facilitating genetic manipulations to investigate adult fat body functions.

Given the central utility of the *GAL4-UAS* system for answering fundamental biological questions with *Drosophila*, our findings emphasize the importance of thoroughly characterizing individual driver lines and thoughtfully selecting genetic reagents when designing experiments. Beyond *Drosophila*, our study contributes to a body of work cautioning potential inadvertent effects of heterologous protein expression in varied biological systems. In *Saccharomyces cerevisiae*, strong expression of eGFP and other fluorescent reporter proteins disrupts proteasomal function and affects cell morphology and growth (Kafri et al. 2016; Kintaka et al. 2016, 2020; Namba et al. 2022; Fujita et al. 2024; Namba and Moriya 2024). Similarly, GFP expressed in cultured cell lines and rodent models can induce apoptosis and elicit deleterious oxidative stress and immunological responses (Liu et al. 1999; Huang et al. 2000; Detrait et al. 2002; Krestel et al. 2004; Agbulut et al. 2006, 2007; Ansari et al. 2016; Kalyanaraman and Zielonka 2017; Verma et al. 2024). Apoptotic neuronal cell death induced by co-expression of eGFP and β-galactosidase in mouse forebrains has been shown to impair motor coordination and cause rapid, early mortality (Krestel et al. 2004). Verma et al. (2024) recently reported severe defects in mouse eye development caused by expression of a Tet-inducible, nuclear-localized GFP reporter construct. Notably, in multiple cases these studies found that higher GFP expression levels, resulting from homozygosity for the transgene or increasing promoter strength, resulted in greater phenotype severity. This aligns with our observations of dose-dependent effects of transgene expression in the *Drosophila* fat body. These prior reports in diverse systems combined with our present work underscore the fact that transgenic proteins employed as experimental "tools" occur within complex, functioning cellular environments, and therefore have the potential to directly or indirectly impact many cellular components and processes. These effects should be empirically evaluated and taken into consideration when designing and interpreting experiments employing the *GAL4-UAS* system and other transgenic systems.

Data availability

Drosophila lines and plasmids are available upon request. The authors affirm that all data necessary for confirming the conclusions of the article are present within the article, figures, and tables.

Supplemental material available at GENETICS online.

Acknowledgments

We are grateful to members of the Lazzaro lab for helpful discussions and advice throughout the completion of this study. We thank Kate Browning for technical assistance with capturing stereoscope images of adult fat bodies. We thank Justin DiAngelo (Penn State Berks) and Alissa Armstrong (University of South Carolina) for sharing fly stocks. We thank Sangbin Park and Seung Kim (Stanford University) for sharing *CyO, LexA-HACKy* + donor flies and providing advice on the HACK approach. Stocks obtained from the Bloomington *Drosophila* Stock Center (NIH P40OD018537) were used in this study.

Funding

This study was supported by National Institutes of Health (NIH) grant R01 AI141385 awarded to BPL. SAK was supported by National Institutes of Health grant T32 AI145821. DVS was supported under a Research Experience for Undergraduates program funded by National Science Foundation grant 1852141.

Conflicts of interest. None declared.

Literature cited

Agbulut O *et al.* 2006. GFP expression in muscle cells impairs actin-myosin interactions: implications for cell therapy. Nat Methods. 3:331. https://doi.org/10.1038/nmeth0506-331.

Agbulut O *et al.* 2007. Green fluorescent protein impairs actin-myosin interactions by binding to the actin-binding site of myosin. J Biol Chem. 282:10465–10471. https://doi.org/10.1074/jbc.M610418200.

Aguila JR, Suszko J, Gibbs AG, Hoshizaki DK. 2007. The role of larval fat cells in adult *Drosophila melanogaster*. J Exp Biol. 210:956–963. https://doi.org/10.1242/jeb.001586.

An W, Wensink PC. 1995a. Integrating sex- and tissue-specific regulation within a single *Drosophila* enhancer. Genes Dev. 9:256–266. https://doi.org/10.1101/gad.9.2.256.

An W, Wensink PC. 1995b. Three protein binding sites form an enhancer that regulates sex-and fat body-specific transcription of *Drosophila* yolk protein genes. EMBO J. 14:1221–1230. https://doi.org/10.1002/j.1460-2075.1995.tb07105.x.

Ansari AM *et al.* 2016. Cellular GFP toxicity and immunogenicity: potential confounders in *in vivo* cell tracking experiments. Stem Cell Rev Rep. 12:553–559. https://doi.org/10.1007/s12015-016-9670-8.

Armstrong AR, Laws KM, Drummond-Barbosa D. 2014. Adipocyte amino acid sensing controls adult germline stem cell number via the amino acid response pathway and independently of target of rapamycin signaling in *Drosophila*. Development. 141:4479–4488. https://doi.org/10.1242/dev.116467.

Arrese EL, Soulages JL. 2010. Insect fat body: energy, metabolism, and regulation. Annu Rev Entomol. 55:207–225. https://doi.org/10.1146/annurev-ento-112408-085356.

Basset A *et al.* 2000. The phytopathogenic bacteria *Erwinia carotovora* infects *Drosophila* and activates an immune response. Proc Natl Acad Sci U S A. 97:3376–3381. https://doi.org/10.1073/pnas.97.7.3376.

Bastock R, St Johnston D. 2008. *Drosophila* oogenesis. Curr Biol. 18:R1082–R1087. https://doi.org/10.1016/j.cub.2008.09.011.

Belote JM, Handler AM, Wolfner MF, Livak KJ, Baker BS. 1985. Sex-specific regulation of yolk protein gene expression in *Drosophila*. Cell. 40:339–348. https://doi.org/10.1016/0092-8674(85)90148-5.

Bownes M. 1994. The regulation of the yolk protein genes, a family of sex differentiation genes in *Drosophila melanogaster*. BioEssays. 16:745–752. https://doi.org/10.1002/bies.950161009.

Bownes M, Blair M. 1986. The effects of a sugar diet and hormones on the expression of the *Drosophila* yolk-protein genes. J Insect Physiol. 32:493–501. https://doi.org/10.1016/0022-1910(86)90011-9.

Bownes M, Ronaldson E, Mauchline D. 1996. 20-Hydroxyecdysone, but not juvenile hormone, regulation of yolk protein gene expression can be mapped to *cis*-acting DNA sequences. Dev Biol. 173:475–489. https://doi.org/10.1006/dbio.1996.0041.

Bownes M, Scott A, As AS. 1988. Dietary components modulate yolk protein gene transcription in *Drosophila melanogaster*. Development. 103:119–128. https://doi.org/10.1242/dev.103.1.119.

Bownes M, Scott A, Blair M. 1987. The use of an inhibitor of protein synthesis to investigate the roles of ecdysteroids and sex-determination genes on the expression of the genes encoding the *Drosophila* yolk proteins. Development. 101:931–941. https://doi.org/10.1242/dev.101.4.931.

Brand AH, Perrimon N. 1993. Targeted gene expression as a means of altering cell fates and generating dominant phenotypes. Development. 118:401–415. https://doi.org/10.1242/dev.118.2.401.

Brankatschk M, Eaton S. 2010. Lipoprotein particles cross the blood-brain barrier in *Drosophila*. J Neurosci. 30:10441–10447. https://doi.org/10.1523/JNEUROSCI.5943-09.2010.

Brennan MD, Weiner AJ, Goralski TJ, Mahowald AP. 1982. The follicle cells are a major site of vitellogenin synthesis in *Drosophila melanogaster*. Dev Biol. 89:225–236. https://doi.org/10.1016/0012-1606(82)90309-8.

Buchon N *et al.* 2013. Morphological and molecular characterization of adult midgut compartmentalization in *Drosophila*. Cell Rep. 3:1725–1738. https://doi.org/10.1016/j.celrep.2013.04.001.

Canavoso LE, Jouni ZE, Karnas J, Pennington JE, Wells MA. 2001. Fat metabolism in insects. Annu Rev Nutr. 21:23–46. https://doi.org/10.1146/annurev.nutr.21.1.23.

Chang KR *et al.* 2022. Transgenic *Drosophila* lines for LexA-dependent gene and growth regulation. G3 (Bethesda). 12:jkac018. https://doi.org/10.1093/g3journal/jkac018.

Chauhan V, Anis A, Chauhan A. 2021. Effects of starvation on the levels of triglycerides, diacylglycerol, and activity of lipase in male and female *Drosophila melanogaster*. J Lipids. 2021:5583114. https://doi.org/10.1155/2021/5583114.

Chippindale AK, Chu TJF, Rose MR. 1996. Complex trade-offs and the evolution of starvation resistance in *Drosophila melanogaster*. Evolution. 50:753–766. https://doi.org/10.1111/j.1558-5646.1996.tb03885.x.

Coschigano KT, Wensink PC. 1993. Sex-specific transcriptional regulation by the male and female doublesex proteins of *Drosophila*. Genes Dev. 7:42–54. https://doi.org/10.1101/gad.7.1.42.

Da Lage J-L, Capy P, David J-R. 1989. Starvation and desiccation tolerance in Drosophila melanogaster adults: effects of environmental temperature. J Insect Physiol. 35:453–457. https://doi.org/10.1016/0022-1910(89)90051-6.

De Gregorio E, Spellman PT, Tzou P, Rubin GM, Lemaitre B. 2002. The toll and imd pathways are the major regulators of the immune response in *Drosophila*. EMBO J. 21:2568–2579. https://doi.org/10.1093/emboj/21.11.2568.

Detrait ER *et al.* 2002. Reporter gene transfer induces apoptosis in primary cortical neurons. Mol Ther. 5:723–730. https://doi.org/10.1006/mthe.2002.0609.

Duffy JB. 2002. GAL4 system in *Drosophila*: a fly geneticist's Swiss army knife. Genesis. 34:1–15. https://doi.org/10.1002/gene.10150.

Duneau DF *et al.* 2017. The toll pathway underlies host sexual dimorphism in resistance to both gram-negative and gram-positive bacteria in mated *Drosophila*. BMC Biol. 15:124. https://doi.org/10.1186/s12915-017-0466-3.

Fleck SA *et al.* 2024. Auxin exposure disrupts feeding behavior and fatty acid metabolism in adult *Drosophila*. eLife. 12:RP91953. https://doi.org/10.7554/eLife.91953.

Fujita Y, Namba S, Moriya H. 2024. Impact of maximal overexpression of a non-toxic protein on yeast cell physiology. eLife. 13:RP99572. https://doi.org/10.7554/eLife.99572.1.

Gandara ACP, Drummond-Barbosa D. 2022. Warm and cold temperatures have distinct germline stem cell lineage effects during *Drosophila* oogenesis. Development. 149:dev200149. https://doi.org/10.1242/dev.200149.

Gavin JA, Williamson JH. 1976. Juvenile hormone-induced vitellogenesis in Apterous4, a non-vitellogenic mutant in *Drosophila melanogaster*. J Insect Physiol. 22:1737–1742. https://doi.org/10.1016/0022-1910(76)90067-6.

Georgel P *et al.* 2001. *Drosophila* immune deficiency (IMD) is a death domain protein that activates antibacterial defense and can promote apoptosis. Dev Cell. 1:503–514. https://doi.org/10.1016/S1534-5807(01)00059-4.

Gibbs AG, Reynolds LA. 2012. *Drosophila* as a model for starvation: evolution, physiology, and genetics. In: McCue MD, editors. Comparative physiology of fasting, starvation, and food limitation. Springer. p. 37–51.

Gupta V, Frank AM, Matolka N, Lazzaro BP. 2022. Inherent constraints on a polyfunctional tissue lead to a reproduction-immunity tradeoff. BMC Biol. 20:1–15. https://doi.org/10.1186/s12915-022-01328-w.

Gutierrez E, Wiggins D, Fielding B, Gould AP. 2007. Specialized hepatocyte-like cells regulate *Drosophila* lipid metabolism. Nature. 445:275–280. https://doi.org/10.1038/nature05382.

Hawkins CJ *et al.* 2000. The Drosophila caspase DRONC is a glutamate/aspartate protease whose activity is regulated by DIAP1, HID and GRIM. J Biol Chem. 275:27084–27093. https://doi.org/10.1074/jbc.M000869200.

Hay BA, Wolff T, Rubin GM. 1994. Expression of baculovirus P35 prevents cell death in *Drosophila*. Development. 120:2121–2129. https://doi.org/10.1242/dev.120.8.2121.

Huang W-Y, Aramburu J, Douglas PS, Izumo S. 2000. Transgenic expression of green fluorescence protein can cause dilated cardiomyopathy. Nat Med. 6:482–483. https://doi.org/10.1038/74914.

Isaac PG, Bownes M. 1982. Ovarian and fat-body vitellogenin synthesis in *Drosophila melanogaster*. Eur J Biochem. 123:527–534. https://doi.org/10.1111/j.1432-1033.1982.tb06563.x.

Jenkins VK, Larkin A, Thurmond J. 2022. Using FlyBase: a database of *Drosophila* genes and genetics. In: Dahmann C, editors. Drosophila: methods and protocols. Humana. p. 1–34.

Jia D, Xu Q, Xie Q, Mio W, Deng W-M. 2016. Automatic stage identification of *Drosophila* egg chamber based on DAPI images. Sci Rep. 6:18850. https://doi.org/10.1038/srep18850.

Johnson MB, Butterworth FM. 1985. Maturation and aging of adult fat body and oenocytes in *Drosophila* as revealed by light microscopic morphometry. J Morphol. 184:51–59. https://doi.org/10.1002/jmor.1051840106.

Jowett T, Postlethwait JH. 1980. The regulation of yolk polypeptide synthesis in *Drosophila* ovaries and fat body by 20-hydroxyecdysone and a juvenile hormone analog. Dev Biol. 80:225–234. https://doi.org/10.1016/0012-1606(80)90510-2.

Juneja P, Lazzaro BP. 2009. *Providencia sneebia sp.* Nov. And *Providencia burhodogranariea sp.* Nov., isolated from wild *Drosophila melanogaster*. Int J Syst Evol Microbiol. 59:1108–1111. https://doi.org/10.1099/ijs.0.000117-0.

Jürgens KJ, Drechsler M, Paululat A. 2024. An anatomical atlas of *Drosophila melanogaster*—the wild-type. Genetics. 228:iyae129. https://doi.org/10.1093/genetics/iyae129.

Kafri M, Metzl-Raz E, Jona G, Barkai N. 2016. The cost of protein production. Cell Rep. 14:22–31. https://doi.org/10.1016/j.celrep.2015.12.015.

Kalyanaraman B, Zielonka J. 2017. Green fluorescent proteins induce oxidative stress in cells: a worrisome new wrinkle in the application of the GFP reporter system to biological systems? Redox Biol. 12:755–757. https://doi.org/10.1016/j.redox.2017.03.019.

Kassambara A, Kosinski M, Biecek P. survminer: Drawing Survival Curves using "ggplot2" (R package version 0.5.0.999). 2024. Accessed 30 October 2024. https://github.com/kassambara/survminer.

Khalil S, Jacobson E, Chambers MC, Lazzaro BP. 2015. Systemic bacterial infection and immune defense phenotypes in Drosophila melanogaster. J Vis Exp. e52613. https://doi.org/10.3791/52613.

Kim C-H, Paik D, Rus F, Silverman N. 2014. The caspase-8 homolog dredd cleaves imd and relish but is not inhibited by p35. J Biol Chem. 289:20092–20101. https://doi.org/10.1074/jbc.M113.544841.

Kintaka R *et al.* 2020. Genetic profiling of protein burden and nuclear export overload. eLife. 9:e54080. https://doi.org/10.7554/eLife.54080.

Kintaka R, Makanae K, Moriya H. 2016. Cellular growth defects triggered by an overload of protein localization processes. Sci Rep. 6:31774. https://doi.org/10.1038/srep31774.

Klepsatel P, Wildridge D, Gáliková M. 2019. Temperature induces changes in *Drosophila* energy stores. Sci Rep. 9:5239. https://doi.org/10.1038/s41598-019-41754-5.

Kramer JM, Staveley BE. 2003. GAL4 causes developmental defects and apoptosis when expressed in the developing eye of *Drosophila melanogaster*. Genet Mol Res. 2:43–47.

Krestel HE, Mihaljevic ALA, Hoffman DA, Schneider A. 2004. Neuronal co-expression of EGFP and β-galactosidase in mice causes neuropathology and premature death. Neurobiol Dis. 17: 310–318. https://doi.org/10.1016/j.nbd.2004.05.012.

Kühnlein RP. 2012. Lipid droplet-based storage fat metabolism in *Drosophila*. J Lipid Res. 53:1430–1436. https://doi.org/10.1194/jlr.R024299.

Lai S-L, Lee T. 2006. Genetic mosaic with dual binary transcriptional systems in *Drosophila*. Nat Neurosci. 9:703–709. https://doi.org/10.1038/nn1681.

Lannan E, Vandergaast R, Friesen PD. 2007. Baculovirus caspase inhibitors P49 and P35 block virus-induced apoptosis downstream of effector caspase DrICE activation in *Drosophila melanogaster* cells. J Virol. 81:9319–9330. https://doi.org/10.1128/jvi.00247-07.

Lazareva AA, Roman G, Mattox W, Hardin PE, Dauwalder B. 2007. A role for the adult fat body in *Drosophila* male courtship behavior. PLoS Genet. 3:e16. https://doi.org/10.1371/journal.pgen.0030016.

Lazzaro BP. 2002. A population and quantitative genetic analysis of the Drosophila melanogaster antibacterial immune response [Ph.D. Thesis]. Pennsylvania State University.

Lee G, Park JH. 2004. Hemolymph sugar homeostasis and starvation-induced hyperactivity affected by genetic manipulations of the adipokinetic hormone-encoding gene in Drosophila melanogaster. Genetics. 167:311–323.

Lei Y *et al.* 2023. FGF signaling promotes spreading of fat body precursors necessary for adult adipogenesis in *Drosophila*. PLoS Biol. 21: e3002050. https://doi.org/10.1371/journal.pbio.3002050.

Lin C-C, Potter CJ. 2016. Editing transgenic DNA components by inducible gene replacement in *Drosophila melanogaster*. Genetics. 203: 1613–1628. https://doi.org/10.1534/genetics.116.191783.

Linder JE, Owers KA, Promislow DEL. 2008. The effects of temperature on host–pathogen interactions in D. *melanogaster*: who benefits? J Insect Physiol. 54:297–308. https://doi.org/10.1016/j.jinsphys.2007.10.001.

Liu H-S, Jan M-S, Chou C-K, Chen P-H, Ke N-J. 1999. Is green fluorescent protein toxic to living cells? Biochem Biophys Res Commun. 260:712–717. https://doi.org/10.1006/bbrc.1999.0954.

Liu Y, Lehmann M. 2008. A genomic response to the yeast transcription factor GAL4 in *Drosophila*. Fly (Austin). 2:92–98. https://doi.org/10.4161/fly.6311.

Ma P *et al.* 2021. Mifepristone (RU486) inhibits dietary lipid digestion by antagonizing the role of glucocorticoid receptor on lipase transcription. iScience. 24:102507. https://doi.org/10.1016/j.isci.2021.102507.

Manseau L *et al.* 1997. GAL4 enhancer traps expressed in the embryo, larval brain, imaginal discs, and ovary of Drosophila.. Dev Dyn. 209:310–332.

McClure CD *et al.* 2022. An auxin-inducible, GAL4-compatible, gene expression system for *Drosophila*. eLife. 11:e67598. https://doi.org/10.7554/eLife.67598.

McGuire SE, Le PT, Osborn AJ, Matsumoto K, Davis RL. 2003. Spatiotemporal rescue of memory dysfunction in *Drosophila*. Science. 302:1765–1768. https://doi.org/10.1126/SCIENCE.1089035.

Meier P, Silke J, Leevers SJ, Evan GI. 2000. The Drosophila caspase DRONC is regulated by DIAP1. EMBO J. 19:598–611. https://doi.org/10.1093/emboj/19.4.598.

Minoo P, Postlethwait J. 1985. Biosynthesis of *Drosophila* yolk polypeptides. Arch Insect Biochem Physiol. 2:7–27. https://doi.org/10.1002/arch.940020103.

Molaei M, Vandehoef C, Karpac J. 2019. NF-κB shapes metabolic adaptation by attenuating foxo-mediated lipolysis in *Drosophila*. Dev Cell. 49:802–810.e6. https://doi.org/10.1016/j.devcel.2019.04.009.

Myllymäki H, Valanne S, Rämet M. 2014. The *Drosophila* imd signaling pathway. J Immunol. 192:3455–3462. https://doi.org/10.4049/jimmunol.1303309.

Namba S, Kato H, Shigenobu S, Makino T, Moriya H. 2022. Massive expression of cysteine-containing proteins causes abnormal elongation of yeast cells by perturbing the proteasome. G3 (Bethesda). 12:jkac106. https://doi.org/10.1093/g3journal/jkac106.

Namba S, Moriya H. 2024. Toxicity of the model protein 3×GFP arises from degradation overload, not from aggregate formation. J Cell Sci. 137:jcs261977. https://doi.org/10.1242/jcs.261977.

Nezis IP, Stravopodis DJ, Papassideri I, Robert-Nicoud M, Margaritis LH. 2002. Dynamics of apoptosis in the ovarian follicle cells during the late stages of *Drosophila* oogenesis. Cell Tissue Res. 307: 401–409. https://doi.org/10.1007/s00441-001-0498-3.

Osterwalder T, Yoon KS, White BH, Keshishian H. 2001. A conditional tissue-specific transgene expression system using inducible GAL4. Proc Natl Acad Sci U S A. 98:12596–12601. https://doi.org/10.1073/pnas.221303298.

Parisi M, Li R, Oliver B. 2011. Lipid profiles of female and male *Drosophila*. BMC Res Notes. 4:198. https://doi.org/10.1186/1756-0500-4-198.

Ramírez-Zacarías JL, Castro-Muñozledo F, Kuri-Harcuch W. 1992. Quantitation of adipose conversion and triglycerides by staining intracytoplasmic lipids with oil red O. Histochemistry. 97: 493–497. https://doi.org/10.1007/BF00316069.

Rankin AE *et al.* 2024. Simplified homology-assisted CRISPR for gene editing in *Drosophila*. G3 (Bethesda). 14:jkad277. https://doi.org/10.1093/g3journal/jkad277.

Rezával C, Werbajh S, Ceriani MF. 2007. Neuronal death in *Drosophila* triggered by GAL4 accumulation. Eur J Neurosci. 25:683–694. https://doi.org/10.1111/j.1460-9568.2007.05317.x.

Robles-Murguia M, Hunt LC, Finkelstein D, Fan Y, Demontis F. 2019. Tissue-specific alteration of gene expression and function by RU486 and the GeneSwitch system. NPJ Aging Mech Dis. 5:6. https://doi.org/10.1038/s41514-019-0036-8.

Shaw AE *et al.* 2012. *Drosophila melanogaster* as a model organism for bluetongue virus replication and tropism. J Virol. 86:9015–9024. https://doi.org/10.1128/jvi.00131-12.

Stronach B, Lennox AL, Garlena RA. 2014. Domain specificity of MAP3 K family members, MLK and Tak1, for JNK signaling in *Drosophila*. Genetics. 197:497–513. https://doi.org/10.1534/genetics.113.160937.

Tarone AM, McIntyre LM, Harshman LG, Nuzhdin SV. 2012. Genetic variation in the yolk protein expression network of *Drosophila melanogaster*: sex-biased negative correlations with longevity. Heredity (Edinb). 109:226–234. https://doi.org/10.1038/hdy.2012.34.

Terashima J, Takaki K, Sakurai S, Bownes M. 2005. Nutritional status affects 20-hydroxyecdysone concentration and progression of oogenesis in *Drosophila melanogaster*. J Endocrinol. 187:69–79. https://doi.org/10.1677/joe.1.06220.

Troha K, Im JH, Revah J, Lazzaro BP, Buchon N. 2018. Comparative transcriptomics reveals CrebA as a novel regulator of infection tolerance in *D. melanogaster*. PLoS Pathog. 14:e1006847. https://doi.org/10.1371/journal.ppat.1006847.

Tsuyama T, Hayashi Y, Komai H, Shimono K, Uemura T. 2023. Dynamic *de novo* adipose tissue development during metamorphosis in *Drosophila melanogaster*. Development. 150:dev200815. https://doi.org/10.1242/dev.200815.

Tzou P *et al.* 2000. Tissue-specific inducible expression of antimicrobial peptide genes in *Drosophila* surface epithelia. Immunity. 13:737–748. https://doi.org/10.1016/S1074-7613(00)00072-8.

Uv AE *et al.* 2000. *Members only* encodes a *Drosophila* nucleoporin required for rel protein import and immune response activation. Genes Dev. 14:1945–1957. https://doi.org/10.1101/gad.14.15.1945.

Vaibhvi V, Künzel S, Roeder T. 2022. Hemocytes and fat body cells, the only professional immune cell types in *Drosophila*, show strikingly different responses to systemic infections. Front Immunol. 13:1040510. https://doi.org/10.3389/fimmu.2022.1040510.

Valanne S, Wang J-H, Rämet M. 2011. The *Drosophila* toll signaling pathway. J Immunol. 186:649–656. https://doi.org/10.4049/jimmunol.1002302.

Verma S, Moreno IY, Gesteira TF, Coulson-Thomas VJ. 2024. Toxicity of nuclear-localized GFP in reporter mice. Sci Rep. 14:24642. https://doi.org/10.1038/s41598-024-75741-2.

Vidal S *et al.* 2001. Mutations in the *Drosophila dTAK1* gene reveal a conserved function for MAPKKKs in the control of rel/NF-κB-dependent innate immune responses. Genes Dev. 15:1900–1912. https://doi.org/10.1101/gad.203301.

Westlake H, Hanson MA, Lemaitre B. 2025. The Drosophila immunity handbook. 1st ed EPFL Press.

Yamada R *et al.* 2017. Mifepristone reduces food palatability and affects *Drosophila* feeding and lifespan. J Gerontol A Biol Sci Med Sci. 72:173–180. https://doi.org/10.1093/gerona/glw072.

Yoder JH. 2012. Abdominal segment reduction. Fly (Austin). 6:240–245. https://doi.org/10.4161/fly.22109.

Yu S, Luo F, Xu Y, Zhang Y, Jin LH. 2022. *Drosophila* innate immunity involves multiple signaling pathways and coordinated communication between different tissues. Front Immunol. 13:905370. https://doi.org/10.3389/fimmu.2022.905370.

Zappia MP, Damschroder D, Westacott A, Wessells RJ, Frolov MV. 2024. The RU486-dependent activation of the GeneSwitch system in adult muscles leads to severe adverse effects in *Drosophila*. G3 (Bethesda). 14:jkae039. https://doi.org/10.1093/g3journal/jkae039.

Zheng H, Yang X, Xi Y. 2016. Fat body remodeling and homeostasis control in *Drosophila*. Life Sci. 167:22–31. https://doi.org/10.1016/j.lfs.2016.10.019.

Zwaan BJ, Bijlsma R, Hoekstra RF. 1991. On the developmental theory of ageing. I. Starvation resistance and longevity in *Drosophila melanogaster* in relation to pre-adult breeding conditions. Heredity (Edinb). 66:29–39. doi:10.1038/hdy.1991.4

Editor: D. Andrew